Molecular and Cellular Neuroscience 109 (2020) 103553

Contents lists available at ScienceDirect

Molecular and Cellular Neuroscience

journal homepage: www.elsevier.com/locate/ymcne

Modelling frontotemporal dementia using patient-derived induced pluripotent stem cells

Georgie Lines[1], Jackie M. Casey[1], Elisavet Preza[1], Selina Wray[*]

Department of Neurodegenerative Disease, UCL Queen Square Institute of Neurology, University College London, 1 Wakefield Street, London WC1N 1PJ, UK

ARTICLE INFO

Keywords:
iPSC
FTD
Tau
Progranulin
C9ORF72
TDP-43

ABSTRACT

Frontotemporal dementia (FTD) describes a group of clinically heterogeneous conditions that frequently affect people under the age of 65 (Le Ber et al., 2013). There are multiple genetic causes of FTD, including coding or splice-site mutations in *MAPT*, *GRN* mutations that lead to haploinsufficiency of progranulin protein, and a hexanucleotide GGGGCC repeat expansion in *C9ORF72*. Pathologically, FTD is characterised by abnormal protein accumulations in neurons and glia. These aggregates can be composed of the microtubule-associated protein tau (observed in FTD with *MAPT* mutations), the DNA/RNA-binding protein TDP-43 (seen in FTD with mutations in *GRN* or *C9ORF72* repeat expansions) or dipeptide proteins generated by repeat associated non-ATG translation of the *C9ORF72* repeat expansion. There are currently no disease-modifying therapies for FTD and the availability of in vitro models that recapitulate pathologies in a disease-relevant cell type would accelerate the development of novel therapeutics. It is now possible to generate patient-specific stem cells through the reprogramming of somatic cells from a patient with a genotype/phenotype of interest into induced pluripotent stem cells (iPSCs). iPSCs can subsequently be differentiated into a plethora of cell types including neurons, astrocytes and microglia. Using this approach has allowed researchers to generate in vitro models of genetic FTD in human cell types that are largely inaccessible during life. In this review we explore the recent progress in the use of iPSCs to model FTD, and consider the merits, limitations and future prospects of this approach.

1. Introduction

It is estimated that approximately 50 million people world-wide are currently living with dementia, a figure that is predicted to reach 152 million by 2050 (https://www.who.int/news-room/fact-sheets/detail/dementia). Frontotemporal dementia (FTD) accounts for up to 15% of dementia cases, and is the second most common cause of dementia in patients below 65 years of age (Bott et al., 2014). Around 40% of FTD cases are familial (Chow et al., 1999), with heritability varying between clinical symptoms (Rohrer et al., 2009). FTD is a clinically, genetically and pathologically heterogeneous disorder. The main clinical subtypes of FTD are behavioral variant FTD (bvFTD) and primary progressive aphasia (PPA), which are characterised by changes in behavior and language deficits respectively (Greaves and Rohrer, 2019). FTD also clinically overlaps with a number of motor disorders including progressive supranuclear palsy (PSP), corticobasal syndrome (CBS), parkinsonian disorders (FTD-PD), and motor-neuron disease (FTD-MND or FTD-ALS) (Rohrer et al., 2009). Multiple genetic causes of familial FTD have been identified. The most common mutations associated with FTD are in the genes encoding the microtubule-associated protein tau; *MAPT* (Clark et al., 1998; Hutton et al., 1998; Poorkaj et al., 1998; Spillantini et al., 1998), progranulin; *GRN* (Baker et al., 2006; Cruts et al., 2006), and *C9ORF72* (Renton et al., 2011; DeJesus-Hernandez et al., 2011). Rarer causative mutations in *VCP* (Watts et al., 2004; Watts et al., 2007), *TARDBP* (Borroni et al., 2009) and *CHMP2B* (Skibinski et al., 2005) have also been identified. The pathology of FTD can be classified according to the constitution of its protein inclusions. FTLD-tau accounts for 30–50% of FTD cases (Baborie et al., 2011; Josephs et al., 2011; Sieben et al., 2012) and is pathologically identified by the presence of tau-positive inclusions which are a hallmark of FTD with *MAPT* mutations (Gotz et al., 2019; Takada, 2015). FTLD-TDP occurs in 50–60% of FTD patients (Baborie et al., 2011; Josephs et al., 2011; Sieben et al., 2012) and displays tau-negative but ubiquitin/TDP-43 positive inclusions. FTLD-TDP pathology is present in cases of FTD with *GRN* mutations (Mackenzie, 2007), *VCP* mutations (Cairns et al., 2007; Neumann et al., 2007), *TARDBP* mutations (Borroni et al., 2010) and *C9ORF72* repeat expansions (Cairns et al., 2007; Rohrer et al., 2011). The third major histological category, FTLD-FUS, occurs in around 10% of FTD cases (Mackenzie et al., 2011). Protein inclusions in FTLD-FUS are tau negative, TDP-43 negative,

* Corresponding author at: Department of Neurodegenerative Disease, UCL Queen Square Institute of Neurology, London WC1N 1PJ, UK.
E-mail address: selina.wray@ucl.ac.uk (S. Wray).
[1] Authors contributed equally.

https://doi.org/10.1016/j.mcn.2020.103553
Received 8 February 2020; Received in revised form 27 August 2020; Accepted 12 September 2020
Available online 19 September 2020

ubiquitin-positive, FUS (fused in sarcoma) positive (Mackenzie and Neumann, 2016).

Overlap in the genetics, clinical symptoms and pathology between FTD and ALS have led to the interpretation that ALS and FTD are two diseases on a single spectrum (Ghosh and Lippa, 2015). Indeed, patients with FTD can develop motor deficits (Le Ber et al., 2013; Greaves and Rohrer, 2019). Lashley et al. have written a thorough overview of the clinical, genetic and pathological heterogeneity in FTD (Lashley et al., 2015). There are currently no disease-modifying treatments for FTD. This may be due, in part, to a lack of disease models that accurately recapitulate the complex pathologies of the disease. Progress towards a disease-modifying therapy would be greatly enhanced by the availability of disease models which reliably recapitulate disease pathologies in the cell type(s) that degenerate in disease.

The ability to reprogram somatic cells into induced pluripotent stem cells (iPSCs) has revolutionised in vitro disease modelling, particularly for neurological disorders where in vitro cultures of human neurons are not available. Briefly, somatic cells such as fibroblasts or peripheral blood mononuclear cells can be taken from a person with a genotype/phenotype of interest, and reprogrammed to a pluripotent state by the exogenous expression of the pluripotency-associated transcription factors Oct4, Klf4, Sox2 and cMyc (Takahashi and Yamanaka, 2006). The resulting iPSCs can be subsequently differentiated into disease-relevant cell types, including multiple subclasses of neurons, astrocytes and microglia, thus permitting the generation of disease models which contain the patient's precise genome in the cell type that selectively degenerates (Fig. 1). These human iPSC-neurons have the advantage of endogenous expression of the mutant gene of interest, in the cell type specifically affected by disease. Here, we will review insights into genetic FTD that have been gained through the use of iPSCs and discuss future directions and challenges.

2. iPSC models of *MAPT* mutations

2.1. Tau pathology and the MAPT gene

Hyperphosphorylated, insoluble aggregates of the microtubule associated protein tau are the pathological hallmark of a range of clinically diverse neurodegenerative diseases collectively termed the tauopathies (Gotz et al., 2019). Alzheimer's Disease (AD) is the most common of these diseases, although AD is widely accepted to be a secondary tauopathy, as genetic and in vivo evidence supports the notion that tau pathology is downstream of amyloid (Gotz et al., 2001; Lewis et al., 2001; Hardy, 2017). Even so, multiple lines of evidence suggest tau dysfunction is essential to neurodegeneration in AD. Tau pathology spreads in a well-defined manner that correlates with clinical severity and the extent of neurodegeneration (Braak and Braak, 1991; Berg et al., 1998; Guillozet et al., 2003; Nelson et al., 2012). Further, tau knockout rodents are largely protected against amyloid toxicity (Rapoport et al., 2002; Roberson et al., 2007; Shipton et al., 2011; Ke et al., 2012). The primary tauopathies, where tau is the defining pathological feature, include progressive supranuclear palsy (PSP), corticobasal degeneration (CBD) and FTD linked to mutations in *MAPT* (Gotz et al., 2019). However, it was the discovery of causative mutations in *MAPT* linked to FTD that provided confirmation that tau dysfunction was sufficient to cause neurodegeneration (Clark et al., 1998; Hutton et al., 1998; Poorkaj et al., 1998; Spillantini et al., 1998).

The tau protein is encoded for by the *MAPT* gene, located on chromosome 17q21.31. *MAPT* consists of 16 exons, and alternative splicing of exons 2, 3, and 10 results in the generation of multiple tau isoforms in the adult CNS. These differ in the inclusion of 0, 1 or 2 N terminal repeats (0N, 1N and 2N), encoded by exons 2 and 3, and in the presence of 3 or 4 C-terminal microtubule binding domains (3R or 4R) encoded by exon 10. Exon 3 is not translated without exon 2, therefore six protein isoforms are generated: 0N3R, 0N4R, 1N3R, 1N4R, 2N3R and 2N4R (Goedert et al., 1989a; Goedert et al., 1989b; Goedert and Jakes, 1990; Andreadis et al., 1995). The levels of 3R and 4R tau are approximately equal in the healthy adult human CNS (Goedert and Jakes, 1990; Kosik et al., 1989).

Over 40 mutations in *MAPT* linked to FTD have been described, and these can either affect the coding sequence or result in altered tau splicing. The majority of mutations are clustered between exons 9–13, within and around the microtubule binding repeats. *MAPT* missense

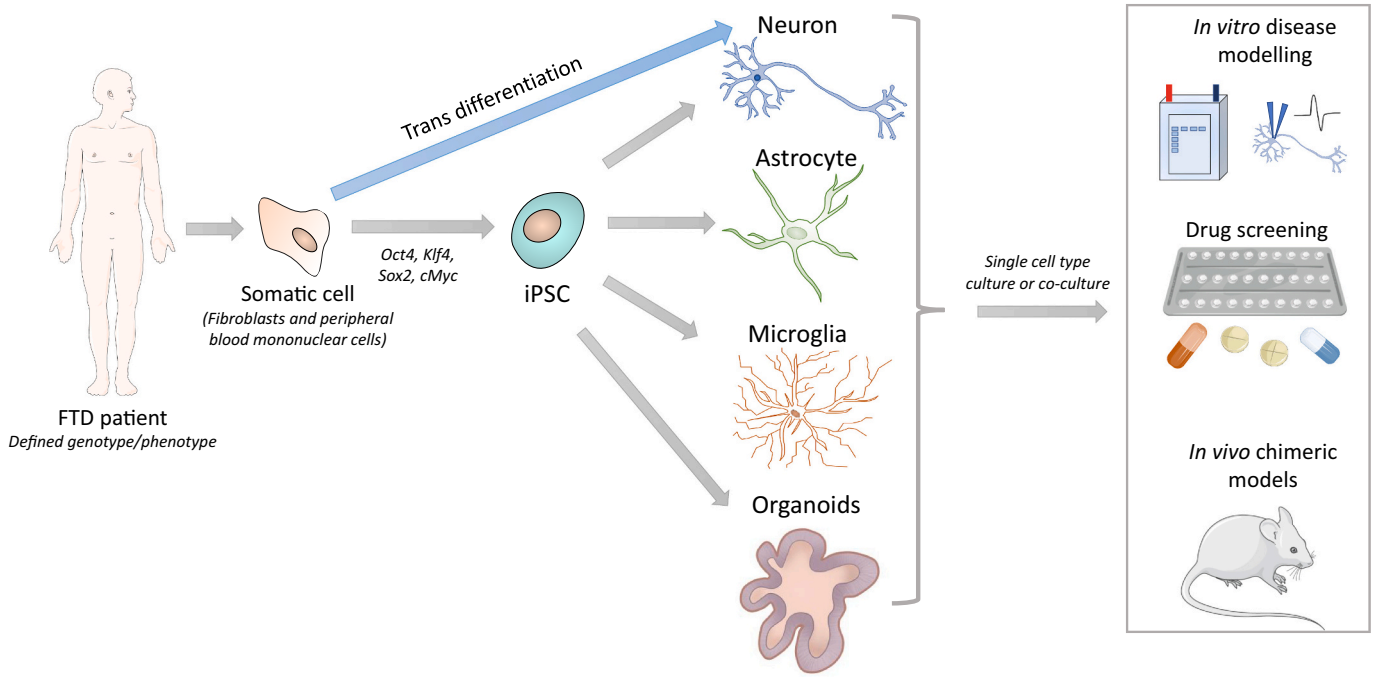

Fig. 1. An overview of iPSC technology.
Somatic cells (such as fibroblasts or PBMCs) can be obtained from patients with genotypes/phenotypes of interest and reprogrammed into iPSCs via the exogenous expression of the transcription factors Oct4, Klf4, Sox2 and cMyc. iPSCs can then be differentiated into multiple cell types affected in FTD, which in turn can be used for disease modelling, drug screening and in vivo chimeric disease modelling. Somatic cells can also be directly converted into neurons via transdifferentiation.

mutations associated with FTD have been identified in exons 1, and 9 to 13. Such mutations (e.g. G272V, P301L, P301S, V337M, R406W) do not influence tau splicing, however they have been shown to decrease the ability of tau to bind to microtubules (Kar et al., 2005) and increase tau aggregation, resulting in neurodegeneration (Rademakers et al., 2004). Mutations located in intron 10 of the *MAPT* gene (10 + 3, 10 + 11, 10 + 12, 10 + 13, 10 + 14, and 10 + 16) cause a dysregulation of *MAPT* splicing. These mutations destabilise a stem loop structure, unmasking the 5′ splice site, resulting in the increased inclusion of exon 10, and an increase in the 4R:3R tau ratio (McCarthy et al., 2015). Additionally, there are a number of mutations present in exon 10 that also disrupt the 4R:3R tau ratio by altering splicing enhancers (N279K) or suppressors (L284L and N296H) (Wszolek et al., 1992; D'Souza et al., 1999; Yasuda et al., 2000; Iseki et al., 2001; Grover et al., 2002). Mutations that cause an imbalance of the 3R/4R tau ratio are sufficient to cause tauopathies (Hutton et al., 1998; Spillantini et al., 1998; McCarthy et al., 2015; Miyamoto et al., 2001), but the mechanisms of how these mutations cause neurodegeneration has not yet been elucidated. The composition of tau pathology in FTD varies depending on the mutation and isoforms affected, and can either consist of all 6 tau isoforms in paired helical filaments, or a subset of isoforms such as 4R-only pathology (Lashley et al., 2015).

The generation of appropriate models to investigate the molecular mechanisms underpinning tauopathies such as FTD has been challenging, as immortalised cell lines and animal models do not recapitulate the complex pattern of *MAPT* splicing seen in the adult human CNS. For example, in the adult murine brain, tau only exists in three isoforms, each with 4R microtubule binding domains (0N4R, 1N4R and 2N4R) (Liu and Gotz, 2013). Additionally, many studies have relied on tau overexpression models to investigate the proteins role in disease, however this can lead to extreme phenotypes, such as the clogging of axons and re-organisation of the neuronal cytoskeleton, which are not truly reflective of endogenous tau expression in disease (Mandelkow et al., 2003). Primary human neurons have been shown to correctly express all tau isoforms, however these are not widely used due to the limited availability of aborted fetal tissue (Deshpande et al., 2008). Thus, iPSC-neurons provide an attractive model system to study the effect of tau mutations at the endogenous level, and a wide range of iPSCs from tauopathy patients are now accessible to the field (Karch et al., 2019).

2.2. Tau splicing in iPSC-neurons

Tau splicing is developmentally regulated, and proper stoichiometry of tau isoforms appears to be critical for neuronal health (Hutton et al., 1998; Grover et al., 1999). In the fetal stages of development, only the shortest tau isoform, 0N3R, is expressed, however in the post-natal CNS, all six isoforms are present (Goedert et al., 1989b; Andreadis et al., 1995).

Multiple studies using comparative transcriptomics have demonstrated that iPSC-neurons closely resemble fetal neurons, at least in terms of global gene expression profiles (Patani et al., 2012; Handel et al., 2016). This raises the question of whether iPSC-neurons express the full complement of tau isoforms present in the adult human brain, and several groups have investigated this. Sposito et al. demonstrated that control iPSC-cortical neurons express mainly the fetal tau isoform (0N3R from D20 to D100) (Sposito et al., 2015). However, neurons cultured for 365 days showed a switch in tau splicing from exclusively 0N3R, to 0N3R, 0N4R, 1N3R and 1N4R. Interestingly, Sposito et al. did not observe the presence of 2N tau, which is the least abundant isoform in the CNS, accounting for only 9% of total tau, although this could be due to sensitivity of the detection method. Other studies have reported the expression of exon-10 containing tau isoforms from 4 to 10 weeks in iPSC-dopaminergic and mixed neuronal populations (Hartfield et al., 2014; Iovino et al., 2015; Iovino et al., 2010; Beevers et al., 2017). These differences in *MAPT* splicing between studies may be driven by the use of different differentiation protocols, neuronal subtype specific regulation of *MAPT* splicing, or differences in the sensitivity of methods used to detect tau. However, these studies have important implications for modelling tauopathies, as they demonstrate that iPSC-neurons have the ability to recapitulate the complex developmental splicing of *MAPT*, and express multiple tau isoforms.

The use of mass spectrometry can provide sensitive and unambiguous identification of tau isoforms. Paonessa et al. reported expression of 3R and 4R tau after 120 days using non-quantitative mass spectrometry (Paonessa et al., 2019). Sato et al. developed a stable isotope labelling kinetics (SILK) quantitative mass spectrometry protocol to examine tau production and turnover (Sato et al., 2018). They demonstrated that iPSC-neurons express lower levels of 4R tau and have a faster tau turnover rate (6 days) when compared to the human brain (23 days). 4R tau and phosphorylated tau was degraded faster than 3R and non-phosphorylated tau in iPSC-neurons, suggesting unique processing of these tau species.

The full impact of differentiation protocol and cell culture conditions remains to be determined. Interestingly, in a chimeric model, whereby human iPSC-neurons are transplanted into mouse frontal cortex, iPSC-neurons express equimolar levels of 3R and 4R tau at 6 months post injection (Espuny-Camacho et al., 2017). This work suggests that iPSC-neurons may mature faster in an in vivo environment, with a combination of cell types and increased structural diversity. Several groups have reported a more mature tau expression profile in 3D cultures, including a 3D neuronal culture derived from immortalised neuronal progenitor cells (Choi et al., 2014), and a 3D iPSC-neuronal system (Miguel et al., 2019).

Several protocols have been established for the culture of 3D organoids from iPSCs (Lancaster and Knoblich, 2014), resulting in self-organising neuronal structures that can recapitulate fetal brain development (Lancaster et al., 2013; Pasca et al., 2015; Xiang et al., 2017; Krefft et al., 2018). It is also possible to directly convert fibroblasts into neurons by the exogenous expression of pro-neuronal transcription factors in a process known as transdifferentiation (Vierbuchen et al., 2010). This has been shown to promote the retention of biological signals of aging, suggesting that transdifferentiated neurons may be more mature than those converted from iPSCs (Mertens et al., 2015). Tau splicing in organoids and neurons generated by transdifferentiation has not yet been investigated.

Despite the apparent fetal nature of iPSC-neurons, they have been successfully used by multiple groups to investigate mutations that affect tau splicing (summarised in Table 1). Multiple studies have shown that iPSC-neurons with intron 10 splicing mutations, 10 + 16 and 10 + 14, express 4R tau isoforms significantly earlier than controls (Sposito et al., 2015; Imamura et al., 2016a; Verheyen et al., 2018). Similar results have been determined in neurons carrying the exon 10 N279K missense mutation, which also increases the 4R:3R tau ratio at early developmental timepoints (Iovino et al., 2015; Ehrlich et al., 2015; Wren et al., 2015). These results indicate that mutations that alter *MAPT* splicing can override the developmental regulation of tau isoforms.

2.3. Investigating mechanisms of tau-mediated neurodegeneration in iPSC-neurons

2.3.1. Tau pathology

Multiple reports have examined neurons with *MAPT* mutations for hallmarks of tau pathology, including hyperphosphorylation, detergent insolubility and formation of aggregates (Fig. 2). Tau phosphorylation has been reported to be significantly higher than controls in iPSC-neurons carrying *MAPT* mutations including 10 + 16, P301L, N279K, and V337M (Iovino et al., 2015; Paonessa et al., 2019; Ehrlich et al., 2015). In all these cases phosphorylation was increased at S202 and T205 (as detected by AT8 antibody), epitopes that are typically hyperphosphorylated in tauopathies (Alonso Adel et al., 2004; Wang

Table 1
Summary of phenotypes identified in studies using *MAPT* mutation iPSC-neurons.

Gene (mutation)	Reference	Cell type	Phenotype				
			↑ 4R tau	↑ Tau phosphorylation	Tau mis-localisation	Accumulation of misfolded, insoluble or aggregated tau species	Additional observations
MAPT (10 + 16)	(Sposito et al., 2015)	Cortical neurons	Y	N	N/A	N/A	• Neurons in extended culture up to 365 days expressed all 6 tau isoforms
	(Paonessa et al., 2019)	Cortical neurons	Y	Y	Y	N	• Mislocalization of tau from axons to cell body and dendrites • Nuclei were more frequently seen with folds and invaginations • Defective nucleocytoplasmic transport
MAPT (10 + 14)	(Imamura et al., 2016a)	Cortical neurons	Y	N/A	N/A	Y	• Sensitivity to electrical stimulation, invoking a larger calcium release compared to controls • Inhibition of calcium influx decreased intracellular and extracellular mis-folded tau, and increased cell survival
MAPT (P301L)	(Iovino et al., 2015)	Cortical neurons	N	Y	N	N	• Earlier electrophysiological maturation and altered mitochondrial transport compared to controls • Contorted processes with varicosity like structures, some containing both alpha-synuclein and 4R tau • Tau localised in cell bodies in both mutant and control cells
MAPT (N279K)	(Wren et al., 2015)	NSC	Y	N/A	N/A	N/A	• Increased stress granules and impaired lysosomal trafficking
	(Ehrlich et al., 2015)	Mixed neurons	Y	Y	N	N	• Increased tau fragmentation • Increased vulnerability to oxidative and ER stress • Decreased neurite length
MAPT (N279K)	(Iovino et al., 2015)	Cortical neurons	Y	Y	N	Y	• Earlier electrophysiological maturation • Decreased anterograde mitochondrial transport • Tau localised in cell bodies in both mutant and control cells
MAPT (A152T)	(Fong et al., 2013)	Mixed neurons	N/A	Y	Y	N/A	• Punctate tau • Short neurites with bulges, constrictions and odd bends, axonal degeneration
	(Silva et al., 2016)	Cortical neurons	N/A	Y	Y	Y	• Accumulation of insoluble phosphorylated tau • Increased autophagy and UPS markers, suggesting proteostasis impairment
MAPT (V337M)	(Ehrlich et al., 2015)	Mixed neurons	N	Y	N	N	• Increased tau fragmentation • Decreased neurite length • Increased vulnerability to cell stress
MAPT (R406W)	(Imamura et al., 2016a)	Cortical neurons	N/A	N/A	N/A	Y	• Sensitivity to electrical stimulation, invoking a larger calcium release compared to controls • Inhibition of calcium influx decreased intracellular and extracellular misfolded tau, and increased cell survival
MAPT (10 + 16, P301L and N279K triple mutant)	(Garcia-Leon et al., 2018)	Cortical neurons	Y	N	Y	Y*	• *Endogenously triggered tau aggregation • Increased electrophysiological activity • Decreased neurite outgrowth Significant activation of stress response pathways

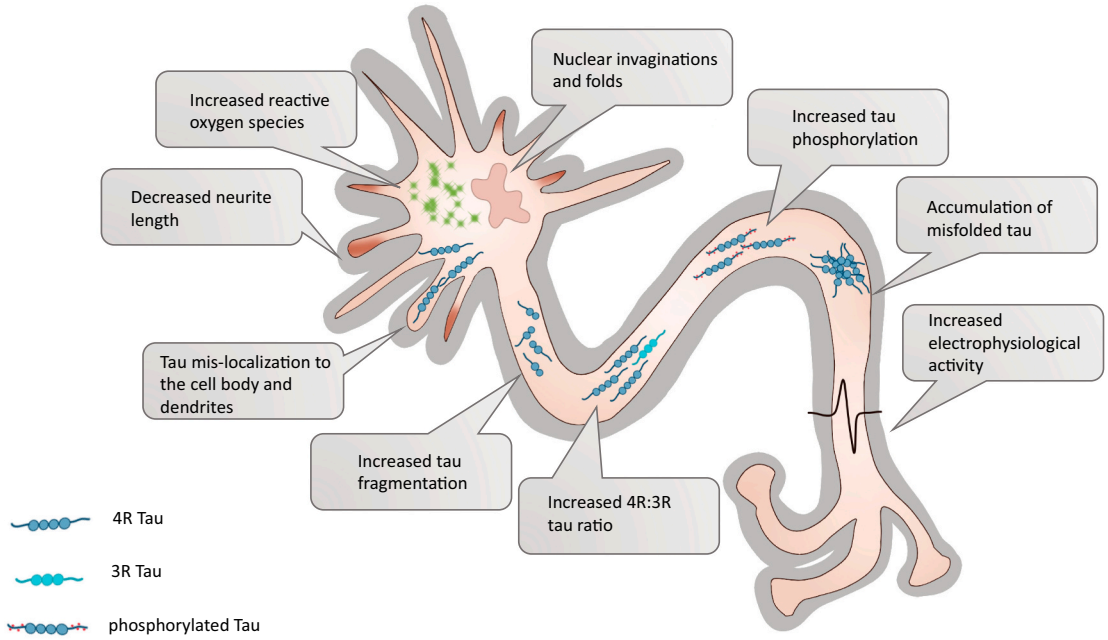

Fig. 2. Common phenotypes observed iPSC-neurons with *MAPT* mutations.
A schematic representation displaying common phenotypes observed in iPSC-cortical neurons with *MAPT* mutations, including nuclear invaginations and folds, increased tau phosphorylation, accumulation of misfolded tau, increased electrophysiological activity, increased 4R:3R tau ratio, increased tau fragmentation, decreased neurite length, and increased reactive oxygen species.

et al., 2013), but not in the developing brain (Hefti et al., 2019). Interestingly Nakamura et al. report that in R406W iPSC-neurons, tau isotopes S404 and S409 are less phosphorylated compared to control neurons (Nakamura et al., 2019). Further investigation revealed that the R406W mutation impaired the phosphorylation of S404 by GSK and CDK5, and S409 by Rho-associated protein kinase and protein kinase A (Nakamura et al., 2019). Tau phosphorylation is also developmentally regulated, and multiple epitopes in human (Hefti et al., 2019) and mouse brain (Yu et al., 2009) show higher phosphorylation at early developmental stages. Thus, it is also important to consider the fetal identity of iPSC-neurons and how this may impact on assigning disease-associated phosphorylation events.

Imamura et al. reported that 10 + 14 and R406W iPSC-neurons displayed an accumulation of intracellular misfolded tau detected using the anti-oligomeric tau antibody, TOC1 (Imamura et al., 2016a). Interestingly, the high molecular weight species observed in 10 + 14 cell lysates, were not the same as those observed in R406W cell lysates. This suggests that the conformation of misfolded tau is not uniform between mutations, which could contribute to the heterogeneity seen in FTD. Iovino et al. demonstrated that iPSC-neurons with N279K mutations displayed occasional dot-like structures when stained with a phosphorylated S212 and S214 antibody (AT100), indicating filamentous tau aggregates. These aggregates were only observed in N279K neurons, not in controls or in P301L mutation neurons (Iovino et al., 2015).

These data collectively demonstrate the ability of iPSC-neurons to model early stages of tau pathology. However, so far the presence of tau tangles in *MAPT* mutation neurons (by Gallyas positive staining or visualisation of tau filaments) has not been demonstrated, even in cell lines where multiple *MAPT* mutations have been engineered (Garcia-Leon et al., 2018).

2.3.2. Tau seeding and spread

Braak and Braak postulated that tau pathology spreads from one brain region to another, contributing to progressive white matter loss, as evidenced by pathology studies which show tau pathology progresses in a predictable sequence that correlates with neurodegeneration and the extent of dementia (Braak and Braak, 1991). This has promoted numerous studies investigating the transcellular spreading of tau in disease, which are reviewed in Demaegd et al. (Demaegd et al., 2018). Recently, iPSCs have begun to be utilized to model tau spread. Tau can be released from wild-type iPSC-neurons into the extracellular space and taken up trans-neuronally by primary neurons (Wu et al., 2016). Evans et al. reported that monomeric wild type and P301S tau, and aggregated P301S tau, can efficiently enter iPSC-neurons by endocytosis, suggesting that tau spread is a biological event, not a necessarily a disease-specific phenomenon (Evans et al., 2018). Interestingly, Sato and colleagues demonstrated that in human iPSC-neurons, newly synthesized tau is truncated and released into the media after 3 days, further suggesting that tau release is a regulated, physiological event (Sato et al., 2018).

2.3.3. Alterations in neuronal morphology

A range of morphological differences have been observed in iPSC-neurons carrying *MAPT* mutations (Fig. 2). P301L neurons exhibited thicker, contorted processes with varicosity structures containing alpha synuclein and 4R tau deposits (Iovino et al., 2015), a feature that could also be observed in post-mortem tissue from the same patient. An increased frequency of nuclear lamina invaginations and folds was observed in 10 + 16 and P301L iPSC-neurons and post mortem tissue from 10 + 16 mutation donors (Paonessa et al., 2019). iPSC-neurons with N279K and V337M mutations displayed significantly shorter neurites compared to controls (Ehrlich et al., 2015). In addition, N279K and V337M neurons showed a significant increase in tau fragmentation at the expense of full-length tau, which may be contributing to the disturbed neurite morphology (Ehrlich et al., 2015).

2.3.4. Transport and function of mitochondria

Tau mis-localisation from the axons, to the cell body and dendrites was reported in iPSC-neurons carrying 10 + 16 and R406W mutations (Paonessa et al., 2019; Nakamura et al., 2019). The primary function of tau is to stabilise microtubules, which are essential for the anterograde and retrograde transport of cargo along the axon (Nogales, 2000). Hyperphosphorylation and redistribution of tau may impede its ability to stabilise microtubules, resulting in an impairment in axonal

transport, and eventually axonal degeneration.

The transport of mitochondria throughout neurons is essential for the maintenance of normal cellular function, as neurons have high energy demands, requiring large amounts of ATP (Schwarz, 2013). As such, disruption of mitochondrial transport, and mitochondria activity in general, have been implicated in the pathogenesis of numerous neurodegenerative diseases (Lin and Beal, 2006). Iovino et al. reported more stationary mitochondria in N279K and P301L neurons, in addition to a reduction in anterogradely moving mitochondria in N279K and P301L neurons by 23% and 15.3% respectively (Iovino et al., 2015). In contrast to this finding, Nakamura et al. observed an increase in mitochondria movement in R406W neurons, with more mitochondria moving in the retrograde direction compared to controls. It has previously been reported that the microtubule binding domain of tau has the ability to inhibit the motility of kinesin and dynein (Dixit et al., 2008). Nakamura et al. therefore suggested that the dissociation of mutant tau from microtubules promotes dynein to become more motile, resulting in increased retrograde transport (Nakamura et al., 2019). Alternatively, differences may be due to unknown molecular effects driven by different tau mutations.

Elevated reactive oxygen species (ROS) can directly damage macromolecules, membranes and organelles which have deleterious consequences on the effected cell. Increased mitochondrial membrane potential was observed in 10 + 16 iPSC-neurons, leading to the overproduction of ROS in mitochondria, oxidative stress and cell death (Esteras et al., 2017). Cell death was prevented by the addition of mitochondrial antioxidants, suggesting that damage caused by mitochondrial ROS is a key facilitator of neurodegeneration. Ehrlich et al. also demonstrated that N279K neurons display a significant increase in the release of lactate dehydrogenase after rotenone treatment, suggesting an increased sensitivity to oxidative stress. This was also confirmed by a reduction in cell death after neurons were treated with antioxidants (Ehrlich et al., 2015).

Biswas et al. reported an increase in MMP-9 and MMP-2, Zn containing proteolytic enzymes, in iPSC-neurons with 10 + 16 and A152T mutations (Biswas et al., 2016). These neurons displayed an increased sensitivity to the cell stressor rapamycin, and treatment of control neurons with MMP-9 and MMP-2 was enough to induce cell death, suggesting MMP-9 and MMP-2 may play a role in neurodegeneration. Interestingly, these results are consistent with a publication (Kaplan et al., 2014) which reports that MMP-9 contributes to neuronal vulnerability in ALS, strengthening the idea that FTD and ALS are two diseases on a single spectrum.

2.3.5. Neuronal function

Neurons carrying the N279K and P301L mutations revealed an earlier neuronal maturation compared to controls (Iovino et al., 2015), suggesting a link between tau dysfunction and neuronal activity. Further evidence for this is provided by Imamura et al., who demonstrated that 10 + 14 neurons evoked an elevated calcium transient compared to controls when stimulated, indicating increased electrical activity of mutant neurons (Imamura et al., 2016a). Additionally, transcriptomic analysis of neurons with the R406W mutation revealed reduced expression of GABA receptors (Jiang et al., 2018). In characterising 10 + 16 and A152T (a risk modifying mutation) iPSC-neurons, Biswas et al. reported that when treated with tetrodotoxin, both mutant cultures exhibited an increased number of neurons that responded with action potentials (Biswas et al., 2016). Tau release from neurons is positively modulated by neuronal activity (Pooler et al., 2013), therefore it is tempting to speculate that earlier, more frequent, and stronger electrical activity of mutant neurons could be contributing to the development and spread of tau pathology.

2.3.6. Modelling tau variants that increase risk of tauopathy

The mutations discussed above (10 + 16, 10 + 14, N279K, V337M, R406W) are all causative of FTD. The A152T variant has recently been shown to increase risk of tauopathy (Kara et al., 2012; Coppola et al., 2012). iPSC-neurons with the A152T variant display prominent neurodegenerative phenotypes, such as increased tau fragmentation and phosphorylation, tau misocalization and axonal degeneration (Zhang et al., 2013; Silva et al., 2016; Silva et al., 2019). It is curious that such strong phenotypes can be observed in relatively young neurons with a variant that is a risk-modifier rather than a causative mutation, however similar phenotypes have also been reported in patients with the A152T mutation (Zhang et al., 2013). It is also possible that cellular phenotypes are exacerbated in vitro due to a lack of other cell types, such as astrocytes, which would normally provide trophic support. Importantly, Silva et al. demonstrated that tau accumulation and phosphorylation phenotypes these phenotypes could be rescued in A152T neurons following the targeted degradation of tau (Silva et al., 2019). In addition Silva et al. showed that degradation of tau prevented cell death of A152T neurons after Aβ(1–42) treatment (Silva et al., 2019).

The *MAPT* gene sits in the largest known region of linkage disequilibrium in the human genome, where two major haplotypes exist: H1 and H2 (Baker et al., 1999). The H1 haplotype confers increased risk for PSP and CBD (Conrad et al., 1997). Both PSP and CBD are characterised by selective deposition of 4R tau isoforms, and therefore it is possible that H1/H2 have haplotype-specific effects on tau expression and splicing (Caffrey et al., 2008; Trabzuni et al., 2012). Beevers et al. demonstrated that mature dopaminergic iPSC-neurons show haplotype differences in *MAPT* expression, with H1 haplotypes expressing 22% higher levels of *MAPT* than H2 (Beevers et al., 2017). No changes in exon 10 expression associated with *MAPT* haplotype were observed.

3. iPSC models of FTD associated with TDP-43 pathology

3.1. TDP-43 pathology and the TARDBP gene

Mutations in *TARDBP*, the gene that encodes Transactive response DNA-binding protein 43 (TDP-43), can cause both ALS and FTD (Borroni et al., 2010; Sreedharan et al., 2008). TDP-43 is a ubiquitously expressed RNA/DNA binding protein, which is the main constituent of the ubiquitinated inclusions found in the cytoplasm and nucleus in the majority of ALS patients and approximately 50% of FTD patients (FTLD-TDP) (Neumann et al., 2006; Arai et al., 2006; Neumann et al., 2009; Nonaka et al., 2009). TDP-43 pathology is found in familial FTD caused by mutations in *GRN*, *C9ORF72*, and *VCP* (Mackenzie, 2007; Cairns et al., 2007; Neumann et al., 2007; Rohrer et al., 2011). Although, *TARDBP* mutations are more commonly associated with ALS, they can also cause FTD (Borroni et al., 2009; Borroni et al., 2010; Floris et al., 2015; Kovacs et al., 2009) and due to the clinical and pathological overlap these models are also relevant to understanding FTD and have therefore been included in this review. TDP-43 inclusions and/or alterations have also been linked to a number of other diseases and injuries, including Alzheimer's Disease, Niemann-Pick C and Traumatic Brain Injury (Amador-Ortiz et al., 2007; Dardis et al., 2016; Jayakumar et al., 2017; McAleese et al., 2017; Wright et al., 2017; Buratti, 2018). TDP-43 can undergo a number of post-translational modifications (PTMs) that affect its function, with the PTM profile and resulting pathology appearing to be disease-specific. Although detection methods limit our identification and knowledge of the effect of certain PTMs, some of the most common disease-associated modifications identified in the ALS/FTD spectrum are; phosphorylation, acetylation, cysteine oxidation, ubiquitination and the generation of C- terminal domains (Buratti, 2018). Phosphorylation of TDP-43 reduces its solubility (Zhang et al., 2010). Cohen et al. found that acetylation resulted in hyper-phosphorylated, aggregated TDP-43, with reduced RNA binding (Cohen et al., 2015). Ubiquitination of TDP-43 has also been found to affect its interaction with p62, which may play a role in clearing TDP-43, with lower rates of coimmunoprecipitation in FTLD-TDP patients than controls (Tanji et al., 2012). C-terminal TDP-43 fragments (25 kDa

and 35 kDa) commonly identified in ALS and FTD lack the nuclear localization signal, which is likely to affect localization and movement between the nucleus and cytoplasm (Buratti, 2018; Ayala et al., 2008).

4. iPSC models of FTD caused by mutations in *GRN*

4.1. GRN mutations in FTD

GRN is located on chromosome 17q21, in the same region as *MAPT*, and codes for the progranulin protein (Baker et al., 2006; Cruts et al., 2006). Mutations in the *GRN* gene that cause haploinsufficiency of progranulin account for 5–10% of all frontotemporal dementia cases (Le Ber et al., 2013) and lead to FTD with TDP-43 pathology (Mackenzie, 2007; Gijselinck et al., 2008; Yu et al., 2010). *GRN* mutations that result in FTD, such as nonsense mutations, splice-site mutations and deletions, have been identified throughout the gene (www.molgen.vib-ua.be/FTDmutations). However, there is significant variability in the age of onset and disease progression, even for patients with the same mutation (Gijselinck et al., 2008; Yu et al., 2010; Gass et al., 2006; Rademakers et al., 2007; Arrant et al., 2018). Progranulin is an 88 kDa secreted glycoprotein, expressed in the brain by both neurons and glia. When progranulin is internalised by cells it can be cleaved to generate seven and a half smaller peptides termed granulins, thought to be the intracellular functional units of progranulin (Kessenbrock et al., 2008; Zhu et al., 2002; Suh et al., 2012; Holler et al., 2017). Multiple functions for progranulin/granulins have been suggested, including the regulation of neuronal differentiation and neurite outgrowth, synaptogenesis, inflammation and wound repair (Zhu et al., 2002; Gao et al., 2010; Yin et al., 2010; Uesaka et al., 2018). More recently, a role for progranulin in lysosome function has emerged. Complete loss of progranulin causes a lysosomal storage disorder, Neuronal Ceroid Lipofuscinosis (NCL) (Smith et al., 2012; Canafoglia et al., 2014; Almeida et al., 2016a). Lysosomal dysfunction is also observed in patients with heterozygous progranulin mutations (Gotzl et al., 2014; Ward et al., 2017), as well as progranulin knock-out mice (Ahmed et al., 2010; Wils et al., 2012). Cleavage of progranulin into the individual granulins is mediated in the lysosome by cathepsins B and L, and progranulin/granulins can regulate the activity of several lysosomal enzymes including glucocerebrosidase (GBA) and cathepsin D (Holler et al., 2017; Jian et al., 2016; Beel et al., 2017; Valdez et al., 2017; Zhou et al., 2017; Butler et al., 2019). Cathepsin D activity is upregulated in $GRN^{-/-}$ mice and pull down assays have identified an interaction between progranulin and cathepsin D (Beel et al., 2017). TDP-43 aggregates have also been detected in mice deficient in cathepsin D and both mice and humans with cathepsin D (CTSD) mutations exhibit symptoms of NCL (Gotzl et al., 2014; Ketscher et al., 2016; Ketterer et al., 2017).

4.2. iPSC-neurons with GRN mutations

4.2.1. Progranulin haploinsufficiency and mislocalised TDP-43 in GRN iPSC-neurons

Almeida et al. generated iPSC-neurons from an FTD patient with a heterozygous *GRN* nonsense mutation (S116X), a healthy control and a sporadic FTD patient (Almeida et al., 2012). *GRN* mRNA was reduced by 41% and intracellular and extracellular progranulin protein levels were reduced by approximately 50% in the *GRN* mutation iPSC-neurons, compared to the healthy and sporadic FTD controls. This demonstrates that patient-derived neurons are a good model of progranulin haploinsufficiency. Mutant GRN iPSC-neurons exhibited an increased sensitivity to tunicamycin and lactacystin, which inhibit protein N-glycosylation and proteasome activity respectively. *GRN* S116X iPSC-neurons also showed increased sensitivity to staurosporine, a broad spectrum kinase inhibitor. Cytoplasmic TDP-43 was increased in the *GRN* S116X iPSC-neurons, in line with previous findings that increased caspase-3 leads to higher levels of cleavage and mislocalisation of TDP-43 (Zhang et al., 2007), demonstrating that iPSC-neurons from *GRN* patients can recapitulate the main disease pathology of *GRN* mutation FTD. These phenotypes were proposed to be due to progranulin haploinsufficiency affecting the PI3K/AKT and MEK/MAPK signaling axis.

4.2.2. Modulating progranulin levels in GRN iPSC-neurons

As all *GRN* mutations result in progranulin haploinsufficiency, methods to restore progranulin levels provide an attractive therapeutic strategy. Several groups have used iPSC-neurons to investigate strategies to upregulate progranulin levels. In Almeida et al.'s (2012) study the increased sensitivity to inhibitors of the PI3K/AKT and MEK/MAPK pathways was rescued by exogenous introduction of *GRN* to restore progranulin levels. A number of follow-up studies used the same iPSC lines as this initial study (Lee et al., 2014; Gascon et al., 2014; Almeida et al., 2016b; Lee et al., 2017). Lee et al. tested methods of preventing binding of progranulin to sortilin (Lee et al., 2014). Sortilin is a neuronal receptor that can internalise progranulin by endocytosis and regulate its trafficking to the lysosome (Hu et al., 2010). They identified amino acids 588–593 of progranulin as the region where sortilin binds and developed small molecules to prevent this interaction, resulting in an increase in extracellular progranulin levels by blocking progranulin uptake. Although this increased extracellular progranulin levels, the impact of reduced lysosomal progranulin/granulins was not explored. Almeida et al. found that 24-hour treatment of 2 week old iPSC-derived cortical neurons with suberoylanilide hydroxamic acid (SAHA) increased levels of *GRN* mRNA and protein in all control, sporadic FTD, and S116X mutation lines without affecting survival rates (Almeida et al., 2016b). Unfortunately, as SAHA is a histone deacetylase inhibitor and affects the expression of many genes, it is unlikely to be suitable as a therapeutic. Another study by Holler et al. found that progranulin was increased in iPSC-neurons treated with trehalose, a disacharride that activates autophagy independently of the mTOR signaling pathway (Holler et al., 2016). Genetic screens in primary neurons and neuroblastoma lines have identified further modifiers of progranulin levels, including *RIPK1* and *TRAP1* (Mason et al., 2017; Elia et al., 2019). The development of CRISPR-based interference screens will enable further identification of genetic modifiers of progranulin levels in human neurons (Tian et al., 2019).

4.2.3. Altered neuronal development and neuronal function in GRN iPSC-neurons

Gascon et al. examined the levels of miR-124 and AMPA receptors (AMPARs) in iPSC lines from a *GRN* (S116X) patient and two *C9ORF72* repeat expansion patients with bvFTD (Gascon et al., 2014). MiR-124 is a small non-coding RNA that plays a role in neural development, and is predicted to target GluA2, GluA3 and GluA4 (Visvanathan et al., 2007; Gao, 2010). Gascon et al. found no difference in miR-124 levels at 2 weeks post differentiation but reduced miR-124 levels and increased GluA2 and GluA4 AMPAR subunits in 8 week old S116X neurons, compared to controls. This would likely result in an increase in Ca^{2+} impermeable AMPARs, as GluA2 subunits are Ca^{2+} impermeable. They also found a decrease in miR-124 levels and associated increases in GluA2 and GluA4 AMPAR subunits in the frontal cortices of patients with sporadic bvFTD and *GRN* haploinsufficiency mutations. They did not detect any difference in NMDA receptors, kainate receptors or miR-9 levels between the groups. Other studies have also found that miR-124 suppresses the expression of GluA2 receptor subunits (Ho et al., 2014; Hou et al., 2015).

Raitano et al. generated iPSCs and then cortical neurons from three patients with a *GRN* (IVS1 + 5G > C) mutation (Raitano et al., 2015). When compared with embryonic stem cells and control iPSCs, they observed less efficient cortical neuronal differentiation in the *GRN* lines, with only a small proportion expressing *TUBB3* mRNA, but no difference in neural progenitor or motor neuron differentiation efficiency. This impairment in cortical neuronal differentiation efficiency was rescued by restoration of progranulin levels. This finding is in

contrast to the initial Almeida et al. study, which found similar rates of differentiation and no difference in the proportion of cells positive for neuronal or astrocytic markers (Almeida et al., 2012). However, Almeida et al. used a protocol to produce a mixed neuronal population and characterised them between 2-4 weeks, whereas Raitano et al. did not identify differences until D40 in vitro and used a protocol to produce predominantly cortical neurons. This could suggest progranulin has a specific role in cortical neuron differentiation.

4.2.4. Lysosomal dysfunction in GRN iPSC-neurons

The lysosomal function of progranulin has gained recent attention and warrants investigation in iPSC models. Lee et al. found that progranulin was localised to the lysosome where it co-localised with cathepsin L, a lysosomal cysteine protease (Lee et al., 2017). Complementary approaches using cathepsin overexpression and pharmacological inhibition support a role of cathepsin L in the cleavage of progranulin into granulins in the lysosome. In addition to being a substrate for cathepsins, progranulin/granulins may also regulate cathepsin maturation and activity. Valdez et al. found decreased cathepsin D activity but no difference in the levels of mature cathepsin D, cathepsin B activity or cathepsin L activity in iPSC-cortical neurons with the A9D *GRN* mutation (Valdez et al., 2017). They identified granulin E, specifically, as an activator of cathepsin D. They also found decreased nuclear TDP-43, along with an increase in insoluble TDP-43. CRISPR/Cas9 correction of the mutation to generate an isogenic control ameliorated these phenotypes. These studies suggest that cathepsin L regulates the levels of full-length progranulin and individual granulins, whereas progranulin regulates cathepsin D activity.

iPSC-derived neurons generated from patients with *GRN* mutations display many of the pathological phenotypes seen in patients (summarised in Table 2 and Fig. 3). To date, these studies have been largely restricted to iPSC-neurons. However, accumulating evidence suggests loss of progranulin disrupts microglia function. Transcriptomics of *GRN* knockout mice revealed specific alterations in microglia that were absent from neurons (Chang et al., 2017) and a further study showed the microglial signature from $GRN^{-/-}$ mice is similar to those isolated from neurodegeneratvive disease brain (Gotzl et al., 2019). Loss of progranulin appears to be associated with altered lipid metabolism, leading to an accumulation of polyunsaturated triacylglycerides in knockout mice (Evers et al., 2017) and a genetic screen idenfified *GRN* as a genetic modifier of lipid droplet formation in microglia (Marschallinger et al., 2020). Future studies investigating the cell-type specific consequences of progranulin haploinsufficiency in iPSC-microglia are eagerly anticipated, and robust protocols have recently been optimised to enable this (Hasselmann and Blurton-Jones, 2020). Further, the contribution of progranulin versus individual granulins to disease aeitiology has not been fully dissected and remains an important knowledge gap for investigation in patient cells.

5. iPSC models of FTD caused by a repeat expansion in *C9ORF72*

The GGGGCC hexanucleotide repeat expansion (HRE) in the first intron of *C9ORF72* is the most common genetic cause of both FTD and amyotrophic lateral sclerosis (ALS) (Renton et al., 2011; DeJesus-Hernandez et al., 2011). The overall mutation frequency of *C9ORF72* is 20% for familial FTD, 16% for familial ALS and around 6%–8% for sporadic ALS and FTD (Marogianni et al., 2019). Unaffected individuals usually carry 2–23 repeats in *C9ORF72*, whereas an arbitrary cut off of 30 repeats is commonly used as the pathogenic repeat size threshold (Rutherford et al., 2012; van der Zee et al., 2013). *C9ORF72* has three main pre-mRNA transcripts (V1, V2 and V3) producing the two main C9ORF72 protein isoforms, a 481amino acid long isoform (C9-L) and a 222 amino acid short isoform (C9-S). C9ORF72 has high homology to Differentially Expressed in Normal and Neoplasia (DENN) related proteins, which act as GDP/GTP exchange factors (GEFs) that activate Rab-GTPases (Levine et al., 2013). Several lines of evidence suggest that

Table 2
Summary of phenotypes identified in studies using *GRN* mutation iPSC derived cells.

Gene (mutation)	Reference	Cell type	Phenotype			
			Progranulin haploinsufficiency	Mislocalised TDP-43	↑ Insoluble TDP-43 or TDP-43 aggregates	Additional observations
GRN (S116X)	(Almeida et al., 2012)	Mixed neurons and microglia	Y	Y	N/A	• Deficits in PI3K/AKT and MEK/MAPK pathways (rescued by increasing progranulin expression)
GRN (S116X) & *C9ORF72* HRE	(Gascon et al., 2014)	Mixed neurons	N/A	N/A	N/A	• Decreased miR-124
GRN (S116X)	(Lee et al., 2014)	Mixed neurons	Y	N/A	N/A	• Increased expression of GluA2 and GluA4 AMPAR subunits • Increased progranulin levels, following inhibition of SORT1 endocytosis
GRN (S116X)	(Almeida et al., 2016b)	Cortical neurons	Y	N/A	N/A	• Increased progranulin after suberoylanilide hydroxamic acid (a histone deacetylase inhibitor)
GRN (S116X)	(Lee et al., 2017)	Mixed neurons	N/A	N/A	N/A	• Cathepsin L cleaves progranulin into individual granulins in the lysosome
GRN (IVS1 + 5G > C)	(Raitano et al., 2015)	Cortical and motor neurons	Y	N	N	• Decreased corticogenesis • Deficits in WNT signaling • Altered gene expression
GRN (R198GfsX19)	(Holler et al., 2016)	Mixed neurons	Y	N/A	N/A	• *GRN* mRNA haploinsufficiency in fibroblasts • Trehalose increased progranulin in patient -derived neurons
GRN (c.26C > A, p.A9D)	(Valdez et al., 2017)	Cortical neurons	Y	Y	Y	• Decreased cathepsin D activity, specifically due to granulin E • Lysosomal dysfunction • Isogenic control line: rescued phenotype

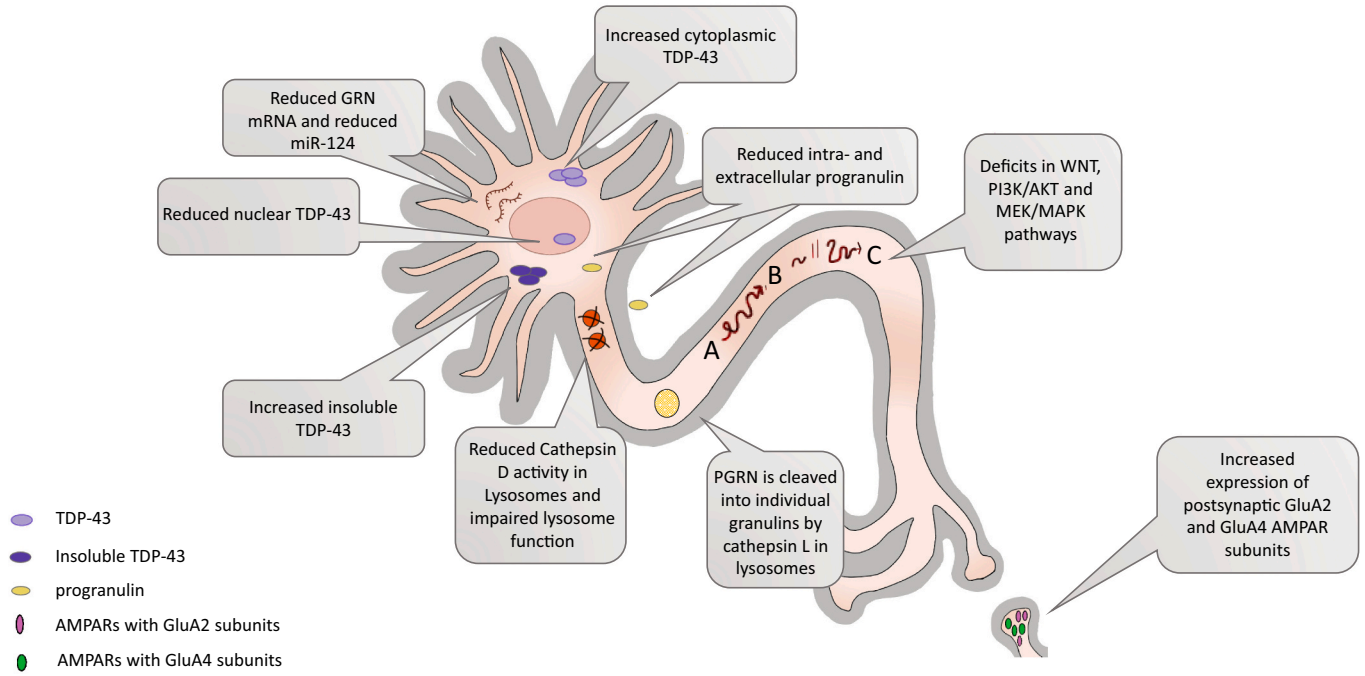

Fig. 3. Common phenotypes observed iPSC-neurons with *GRN* mutations.
A schematic representation displaying common phenotypes observed in iPSC-cortical neurons with *GRN* mutations. These include; reduced intracellular and extracellular progranulin protein, reduced *GRN* mRNA, reduced nuclear TDP-43, increased insoluble and cytoplasmic TDP-43, impaired lysosomal function, reduced Cathepsin D activity, reduced miR-124 and increased expression of GluA2 and GluA4 AMPAR subunits. Deficits in WNT signaling, PI3K/AKT pathways and MEK/MAPK pathways have also been also been identified, as well as the cleavage of progranulin into individual granulins by cathepsin L at the lysosome.

C9ORF72 is involved in autophagy and lysosomal trafficking (Farg et al., 2014; Webster et al., 2016; Sellier et al., 2016; O'Rourke et al., 2016; Sullivan et al., 2016; Yang et al., 2016; Ugolino et al., 2016; Amick et al., 2016; Aoki et al., 2017) but little is known about the distinct functions of the two C9ORF72 protein isoforms. The *C9ORF72* HRE is located in the first intron of *C9ORF72* and following transcription and alternative splicing, V1 and V3 transcripts contain the intronic repeat, but not V2, resulting in different potential pathogenic mechanisms. Studies on *C9ORF72* HRE patient tissue have shown that the HRE leads to (i) a reduction in *C9ORF72* mRNA V2 transcript (DeJesus-Hernandez et al., 2011; Gijselinck et al., 2012; van Blitterswijk et al., 2015), (ii) the formation of sense and antisense RNA foci, produced via bi-directional transcription of the *C9ORF72* HRE from transcripts V1 and V3, which may subsequently sequester RNA-binding proteins (Renton et al., 2011; DeJesus-Hernandez et al., 2011; Lee et al., 2013), and (iii) the production of aggregation-prone dipeptide repeat proteins (DPRs) via repeat-associated, non-ATG (RAN) translation of both sense and anti-sense expanded RNA transcripts in all reading frames (Gly-Ala, Gly-Pro, Pro-Ala, Gly-Arg and Pro-Arg) (Ash et al., 2013; Mori et al., 2013; Gendron et al., 2013). These findings altogether have led to the hypothesis that *C9ORF72* HRE causes FTD/ALS by three potential mechanisms; loss of C9ORF72 function, toxic gain of RNA function or toxic gain of DPR function respectively.

Using iPSCs to model the underlying molecular aetiology of the *C9ORF72* repeat expansion is an attractive approach, as it offers the advantage of fully recapitulating the pathological repeat expansion size present in *C9ORF72* HRE carriers. Nonetheless, it is also challenging as similar to other repeat expansions, the *C9ORF72* HRE is prone to genomic instability (Nordin et al., 2015) leading to HRE mosaicism which is an additional source of genetic heterogeneity in iPSC cultures. Examples of HRE genomic instability and subsequent mosaicism in cell cultures are evident across published *C9ORF72* iPSC studies (Almeida et al., 2013; Sareen et al., 2013; Dafinca et al., 2016; Esanov et al., 2016; Bardelli et al., 2020). Moreover, all three potential disease mechanisms leading to neurodegenerative phenotypes co-exist in patient-derived iPSC models, and although this adds to their physiological relevance, the contribution of each to cellular phenotypes cannot be easily dissected. Here, we provide a comprehensive review of *C9ORF72* iPSC studies and their findings, which are also summarised in Table 3 and illustrated in Fig. 4.

5.1. Capturing the pathology of C9ORF72 FTD in iPSC-neurons

Since the discovery of *C9ORF72* gene as the major genetic cause of FTD/ALS almost a decade ago, several iPSC studies have emerged that recapitulate some of the major pathological hallmarks of C9-FTD/ALS. Multiple groups have shown the presence of sense and/or antisense RNA foci in the nuclei of *C9ORF72* patient-derived cortical neurons (Almeida et al., 2013; Simone et al., 2018; Yuva-Aydemir et al., 2019), mixed neurons (Donnelly et al., 2013), motor neurons (MNs) (Sareen et al., 2013; Dafinca et al., 2016; Simone et al., 2018; Lopez-Gonzalez et al., 2016; Selvaraj et al., 2018; Ababneh et al., 2020) and astrocytes (Zhao et al., 2020). Importantly, some of these iPSC studies have demonstrated that RNA foci can sequester RNA binding proteins such as RNA-editing deaminase-2 (ADARB2) (Donnelly et al., 2013), heterogeneous nuclear ribonucleoprotein A1 (hnRNPA1) and purine-rich binding protein-α (Pur-α) (Sareen et al., 2013) as well as other proteins such as Ran GTPase activating Protein 1 (RANGAP1) (Zhang et al., 2015). It is not known whether this expanded RNA-mediated toxicity is the major driver of neurodegeneration in C9-FTD/ALS similar to what is known for the sequestration of muscleblind proteins by the CUG repeats in myotonic dystrophy (Jiang et al., 2004).

In addition to the presence of RNA foci, DPRs have been identified in iPSC-neurons by multiple studies (Almeida et al., 2013; Dafinca et al., 2016; Simone et al., 2018; Yuva-Aydemir et al., 2019; Donnelly et al., 2013; Lopez-Gonzalez et al., 2016; Ababneh et al., 2020; Zhao et al., 2020). Evidence for cell-to-cell transmission of DPRs was provided by Westergard et al. who showed transmission of poly-GA and poly-GR to control spinal MNs using co-cultures and conditioned media from *C9ORF72* patient-derived spinal MNs (Westergard et al., 2016).

Table 3
Summary of phenotypes identified in studies using *C9ORF72* iPSC-neurons.

Gene (mutation)	Reference	Cell type	Phenotype			
			RNA foci	DPRs	Reduced *C9ORF72* expression	Additional observations
C9ORF72 $(GGGGCC)_n$	(Almeida et al., 2013)	Cortical neurons	Y	Y	Y	• Increased p62 • Compromised autophagy
	(Donnelly et al., 2013)	Mixed neurons	Y	Y	Y	• Sequestration of RNA binding proteins by the expanded RNA • Validation of ADARB2 interaction • Aberrant gene expression • Susceptibility to glutamate excitotoxicity
	(Sareen et al., 2013)	Motor neurons	Y	N	N	• RNA foci colocalisation with hnRNPA1 and Pur-α • Aberrant gene expression • Reduced excitability
	(Meyer et al., 2014)	Induced astrocytes	N/A	N/A	N/A	• Non cell autonomous toxicity of induced astrocytes to co-cultured mouse MNs
	(Wainger et al., 2014)	Motor neurons	N/A	N/A	N/A	• Hyperexcitability • Kv7 channel activator retigabine blocked the hyperexcitability
	(Devlin et al., 2015)	Motor neurons	Y	N/A	N/A	• No changes in cell viability • Initial hyperexcitability followed by a progressive loss in action potential output and synaptic activity
	(Zhang et al., 2015)	Motor neurons	Y	N/A	N/A	• Mislocalisation of RanGAP1 and interaction with HRE RNA • Disrupted nuclear-cytoplasmic pattern of Ran • RanGAP1 overexpression rescued Ran pattern • Abnormal nuclear/cytoplasmic ratio of TDP-43 • Impaired nucleocytoplasmic transport
	(Freibaum et al., 2015)	Cortical neurons	N/A	N/A	N/A	• RNA nuclear export defect, retention of RNA in nuclei • ~ 35% increase in the nuclear/cytoplasmic ratio of RNA density
	(Jovicic et al., 2015)	Induced neurons	N/A	N/A	N/A	• Reduction in nuclear localization of RCC1
	(Esanov et al., 2016)	Motor neurons	N/A	N/A	N/A	• Reduced 5mC levels (methylation) in *C9ORF72* promoter during reprogramming and re-acquiring upon neuronal specification • Increased 5hmC levels (hydroxymethylation) in *C9ORF72* promoter in iPSCs and MNs
	(Cohen-Hadad et al., 2016)	NPCs, teratomas	N/A	N/A	N	• *C9ORF72* promoter hypermethylated in *C9ORF72* HRE iPSC lines but unmethylated in *C9ORF72* HRE ESCs • Increased levels of intron 1-retaining *C9ORF72* transcripts in NPCs and teratomas from *C9ORF72* HRE ESCs compared to those derived from iPSCs
	(Dafinca et al., 2016)	Cortical neurons, motor neurons	Y	Y	N/A	• Increased ER calcium levels • Reduced mitochondrial membrane potential • Reduced levels of the anti-apoptotic protein Bcl-2 • Increased susceptibility to apoptosis • Elevated p62 levels • Abnormal protein aggregation and stress granule formation
	(Westergard et al., 2016)	Motor neurons	N/A	Y	N/A	• Cell-to-cell transmission of DPRs • Transmission of poly-GA and poly-GR aggregates but not poly-GP from *C9ORF72* to control MNs in both co-culture and via conditioned media
	(Ferraiuolo et al., 2016)	Oligodendrocytes	N/A	N/A	N/A	• Patient-derived oligodendrocytes induced MN death in both co-cultures and via oligodendrocyte conditioned media

(*continued on next page*)

Table 3 (*continued*)

Gene (mutation)	Reference	Cell type	Phenotype			
			RNA foci	DPRs	Reduced *C9ORF72* expression	Additional observations
	(Lopez-Gonzalez et al., 2016)	Motor neurons	Y	Y	N/A	• Mitochondrial dysfunction • Age-dependent increase in oxidative stress and DNA damage • Toxicity caused by poly-GR
	(Sivadasan et al., 2016)	Motor neurons	N/A	N/A	Y	• Increased phosphorylation of cofilin in *C9ORF72*-depleted MNs of patients vs controls • C9ORF72 modulated activity of small GTPases Arf6 and Rac1, resulting in increased activity of LIM-kinases 1 and 2 (LIMK1/2) and reduced axonal actin dynamics in C9ORF72-depleted patient MNs • Dominant negative Arf6 reversed phenotype suggesting C9ORF72 acts as a modulator of small GTPases to regulate axonal actin dynamics
	(Aoki et al., 2017)	Motor neurons	N/A	N/A	Y	• Deficits in extracellular vesicle secretion, endosome formation and trans-Golgi network
	(Imamura et al., 2017)	Motor neurons	N/A	N/A	N/A	• Increased survival in *C9ORF72* MNs following treatment with bosutinib, a Src/c-Abl inhibitor
	(Coyne et al., 2017)	Motor neurons	N/A	N/A	N/A	• Impaired synaptic vesicle cycling due to posttranscriptional reduction in the levels of the Hsc70–4/HSPA8 chaperone • HSPA8 levels were reduced in the soma and dendrites of *C9ORF72* MNs by 57% and 32%, respectively
	(Simone et al., 2018)	Cortical neurons, motor neurons	Y	Y	N/A	• Reduction in RNA foci (CNs and MNs) and poly-GP levels (MNs) following treatment with small molecules that bind *C9ORF72* HRE G-quadruplex RNA
	(Selvaraj et al., 2018)	Motor neurons	Y	Y	N	• No difference in excitability • Increased GluA1 AMPAR expression leading to enhanced vulnerability to excitotoxicity • Excision of the HRE resulted in reversal of RNA foci and vulnerability to excitotoxicity phenotypes
	(Shi et al., 2018)	Motor neurons	N/A	N/A	Y	• Reduced survival of patient-derived MNs • Interaction of C9ORF72 with endosomes • C9ORF72 was required for normal vesicle trafficking and lysosomal biogenesis in MNs • Low C9ORF72 activity sensitised MNs to glutamate and DPR toxicity suggesting a synergistic effect between gain and loss of function mechanisms • C9ORF72 restoration, constitutively active RAB5 or small molecule modulators of vesicle trafficking all rescued patient MN survival
	(Moore et al., 2019)	Motor neurons	N/A	N/A	N/A	• Mislocalisation of RNA editing enzyme adenosine deaminase acting on RNA 2 (ADAR2) to the cytoplasm
	(Cheng et al., 2019)	Motor neurons	N/A	Y	N/A	• Glutamate-induced excitotoxicity • Disrupted Ran gradient and nucleocytoplasmic transport • Increased RNA helicase DDX3X levels led to reduction in DPRs, rescuing *C9ORF72* HRE phenotypes of glutamate-induced excitotoxicity and disrupted nucleocytoplasmic transport
	(Yuva-Aydemir et al., 2019)	Cortical neurons	Y	Y	N/A	• Axonal degeneration • Partially cytoplasmic TDP-43 • Transcription elongation factor AFF2/FMR2 regulates the transcription of the HRE

(*continued on next page*)

Table 3 (*continued*)

Gene (mutation)	Reference	Cell type	Phenotype			
			RNA foci	DPRs	Reduced *C9ORF72* expression	Additional observations
						• AFF2 knockout resulted in decreased expression of the *C9ORF72* allele containing the HRE, rescue of axonal degeneration and TDP-43 mislocalisation
	(Birger et al., 2019)	Astrocytes	N/A	N/A	N/A	• Increased oxidative stress • *C9ORF72* astrocyte conditioned media was neurotoxic by inducing oxidative stress in control MNs
	(Zhao et al., 2020)	Astrocytes	Y	Y	N	• Cell-autonomous astrocyte pathology reversed upon CRISPR/Cas-9-mediated excision of the HRE • Progressive loss of action potential output in co-cultured control MNs which was reversed upon CRISPR/Cas-9-mediated excision of the HRE • Phenotypes only present in control MNs co-cultured with *C9ORF72* patient-derived astrocytes and not in *C9ORF72* patient-derived MN-enriched cultures alone (non-cell-autonomous mechanisms)
	(Andrade et al., 2020)	Motor neurons	N/A	N/A	N/A	• Increased DNA damage marker γH2AX • Increased RAD5 (component of the SSA repair machinery) and phosphorylated RAD52 • CRISPR/Cas-9-mediated excision of the HRE resulted in reduction of RAD52 hyperactivation
	(Abo-Rady et al., 2020)	Motor neurons	N/A	Y	N/A	• Axonal transport defects • Reduced levels of ubiquitously expressed chaperone HSP70 • Altered stress granule formation • Phenotypes were exacerbated in isogenic *C9ORF72* patient-derived MNs that contained the HRE as well as a *C9ORF72* knockout, supporting a combination of gain and loss of function mechanisms in C9-ALS/FTD pathogenesis
	(Porterfield et al., 2020)	Cortical neurons 3D	N/A	N/A	N/A	• Spontaneous re-expression of cyclin D1 at 12 weeks post-differentiation, suggesting cell cycle re-engagement • Increased expression of senescence-associated genes including CXCL8, a chemokine overexpressed by senescent cells • Increased levels of components of the senescence-associated secretory phenotype were present in media from *C9ORF72* neurons
	(Ababneh et al., 2020)	Motor neurons	Y	Y	N	• 5′ CpG island hypermethylation in *C9ORF72* MNs • Retention of the HRE-containing intron in *C9ORF72* MNs • Susceptibility of in *C9ORF72* MNs to apoptotic cell death and toxicity • Reversal of all pathological phenotypes and restoration of *C9ORF72* expression and methylation levels upon CRISPR/Cas9-mediated excision of the HRE in isogenic MNs
	(Ratti et al., 2020)	Motor neurons	N/A	N/A	N/A	• Chronic sodium arsenite treatment induced recruitment of TDP-43 into stress granules, formation of distinct cytoplasmic inclusions of phosphorylated TDP-43 and p62 aggregates in *C9ORF72* MNs

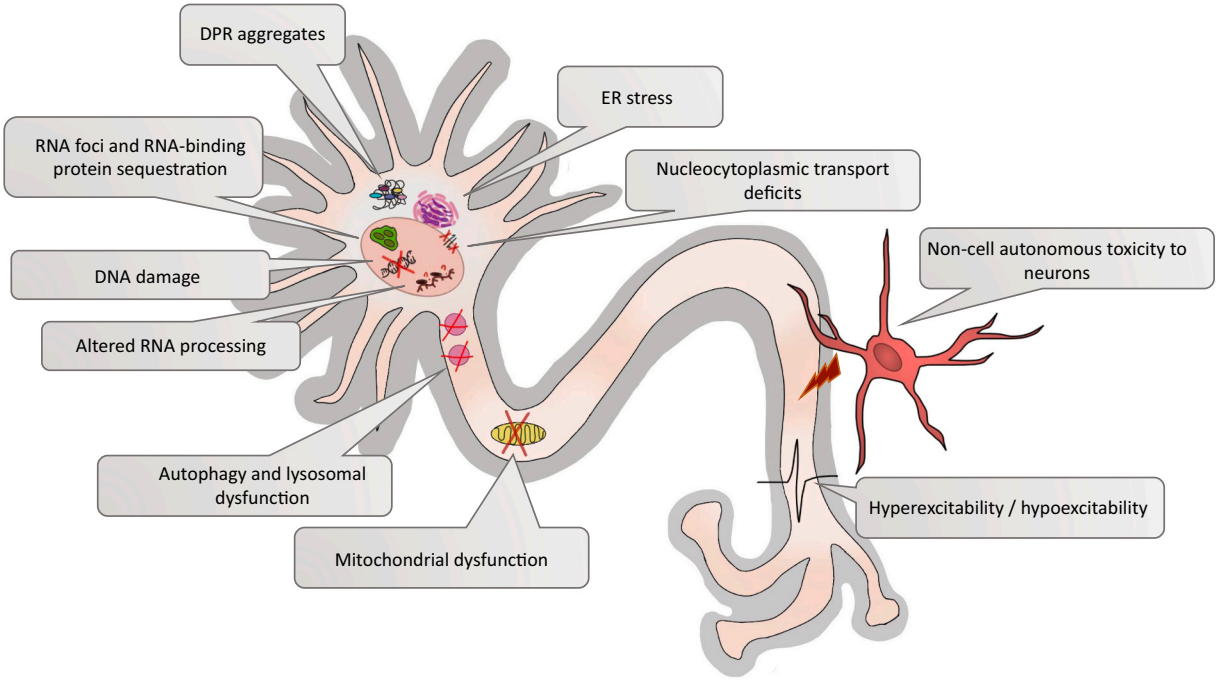

Fig. 4. Common phenotypes observed iPSC-neurons with *C9ORF72* mutations.
A schematic representation displaying common phenotypes observed in iPSC-neurons from patients carrying the *C9ORF72* HRE including intranuclear RNA foci that sequester RNA-binding proteins, DNA damage, nucleocytoplasmic transport defects, DPR aggregates, vulnerability to ER stress and excitotoxicity, mitochondrial dysfunction, compromised autophagy, lysosomal dysfunction and impaired excitability. Non-cell-autonomous toxicity from patient-derived astrocytes and oligodendrocytes has also been demonstrated.

Finally, *C9ORF72* haploinsufficiency has also been observed in *C9ORF72* HRE neurons via a reduction in *C9ORF72* transcript expression (Almeida et al., 2013; Donnelly et al., 2013) or in C9ORF72 protein levels (Aoki et al., 2017; Shi et al., 2018; Sivadasan et al., 2016). Loss of *C9ORF72* can be caused epigenetically due to the presence of the CpG-rich HRE via extensive DNA methylation of CpG residues at the promoter region of the gene. Indeed, hypermethylation of the *C9ORF72* promoter region, consisting of the *C9ORF72* HRE and its flanking CpG

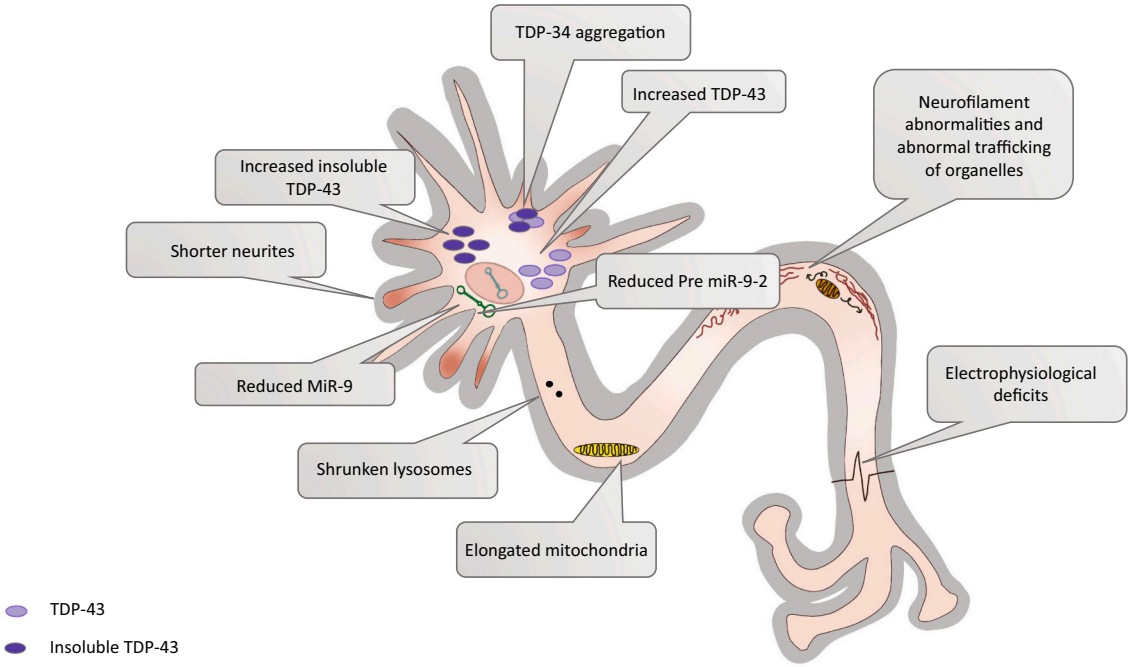

Fig. 5. Common phenotypes observed iPSC-neurons with *TARDBP* mutations.
A schematic representation displaying phenotypes observed in iPSC-cortical neurons with *TARDBP* mutations. These include; increased insoluble and cytoplasmic TDP-43, TDP-43 aggregation, shorter neurites, shrunken lysosomes, reduced miR-9 and pre miR-9-2, initial hyperexcitability followed by a loss of electrophysiological signal, neurofilament abnormalities and abnormal trafficking of organelles.

Table 4
Summary of phenotypes identified in studies using *TARDBP* mutation iPSC-neurons and astrocytes.

Gene (mutation)	Reference	Cell type	Phenotype			
			Aggregated TDP-43	Mislocalised TDP-43	↑ Insoluble TDP-43	Additional observations
TARDBP (M337V)	(Bilican et al., 2012)	Motor neurons and caudalised neurons	N/A	Y	Y	• Increased total TDP-43 • Decreased survival of patient MNs • Increased sensitivity to PI3K inhibitors
TARDBP (M337V)	(Serio et al., 2013)	Astrocytes	N	Y	N	• Increased soluble TDP-43
TARDBP (M337V & A90V)	(Zhang et al., 2013)	Mixed neurons	N/A	N	N	• Decreased total TDP-43 in A90V neurons • Increased TDP-43 mislocalisation in patient lines following staurosporine treatment.
TARDBP (M337V, Q343R and G298S)	(Egawa et al., 2012)	Motor neurons	Y	Y	Y	• TDP-43 binding with SNRPB2 (a spliceosomal factor) • Shorter neurites • Phenotype rescued with anacardic acid (a histone acetyltransferase inhibitor)
TARDBP (A315T)	(Burkhardt et al., 2013)	Motor and cortical neurons	N	N/A	N/A	• Increased levels of TDP-43 and • Detected TDP-43 aggregates in MNs from sporadic ALS patients • Decreased aggregation following treatment with; cyclin- dependent kinase inhibitors, c-Jun N- terminal kinase inhibitors (JNK), Triptolide and FDA- approved cardiac glycosides, Digoxin, Lanatoside C, and Proscillaridin A
TARDBP (M337V)	(Yang et al., 2013)	Motor neurons	N/A	N/A	N/A	• Decreased survival of patient MNs • Kenpaullone (a multikinase inhibitor) significantly improved MN survival
TARDBP (M337V) & *C9ORF72* HRE	(Devlin et al., 2015)	Motor neurons	N/A	N/A	N/A	• Initial hyperexcitability followed by progressive loss of action potential output and synaptic activity • No changes in cell viability
TARDBP (A382T)	(Bossolasco et al., 2018)	Motor neurons	N	N	N/A	• No difference in TDP-43 levels, compared to controls
TARDBP (S393L and G294V)	(Kreiter et al., 2018)	Motor neurons	N	N	N/A	• Abnormal trafficking, mitochondria and lysosomes (D-sorbitol rescued trafficking deficits) • Decreased survival of patient MNs

Table 5
Advantages and limitations of using iPSC-derived cells to model FTD.

Advantages	Limitations
• Production of disease relevant and species-specific cell types. • Endogenous expression of mutant genes of interest. • Expansive resources of iPSCs with a range of FTD mutations available • Range of accessible protocols that yield a high volume of cells which is beneficial for screening assays. • Induction of iPSCs into neurons is developmentally comparable to in vivo neurogenesis. • Models have been shown to reflect select number of phenotypes present in patients. • The ability to investigate cellular mechanisms in iPSC derived models alongside tracking patient progress from which the iPSCs were derived.	• Inter and intra variability in iPSCs linked to genetic heterogeneity • iPSC derived models do not recapitulate all phenotypes observed in disease • Often only looking at a single cell type which limits biological relevance. • Cost of iPSC culture, and the time it takes to mature cells may be prohibitive. • iPSC-neurons are fetal in nature which poses problems for investigating diseases associated with aging.

islands, is a frequent finding in patient brain and blood (Xi et al., 2013; Xi et al., 2014; Belzil et al., 2014; Xi et al., 2015) and has been reported as a disease modifier in ALS/FTD (Russ et al., 2015). To date, only a limited number of studies have assessed DNA methylation in *C9ORF72* HRE iPSC models (Esanov et al., 2016; Ababneh et al., 2020; Cohen-Hadad et al., 2016). The first iPSC study to assess DNA methylation and hydroxymethylation at the *C9ORF72* promoter reported a reduction in 5-methylcytosine (5mC) levels during reprogramming and re-acquiring upon neuronal specification, alongside an increase in 5-hydroxymethylcytosine (5hmC) levels following reprogramming with elevated levels present in iPSCs and MNs (Esanov et al., 2016). However, the use of one patient line and the considerable heterogeneity due to different HRE sizes within and between cellular populations of different developmental stages require cautious interpretation of the results.

Cohen-Hadad et al. assessed DNA methylation at the *C9ORF72* HRE and the upstream 5′ CpG island (*C9ORF72* promoter region) in differentiated neural precursors and teratomas derived from *C9ORF72* HRE human embryonic stem cell (hESC) and iPSC lines (Cohen-Hadad et al., 2016). The 5′ CpG and the HRE itself were found to be hypermethylated in the *C9ORF72* HRE iPSC-NPCs and teratomas. Despite the considerable difference in the HRE size between the iPSC and hESC lines, the authors concluded that reprogramming leads to hypermethylation of the *C9ORF72* promoter region in iPSCs which may lead to milder phenotypes in iPSCs compared to ESCs. This is supported by the finding of increased intron 1-retaining *C9ORF72* transcripts in NPCs and teratomas differentiated from *C9ORF72* HRE hESCs compared to iPSCs. The DNA methylation status of the 5′ CpG island upstream of the HRE was also assessed in a recent study (Ababneh et al., 2020). The authors reported hypermethylation of the 5′ CpG island, increased intron 1-retaining *C9ORF72* transcripts as well as a reduction in total, V1 and V2 *C9ORF72* RNA in iPSC-MNs from one patient which were all restored following CRISPR/Cas9 isogenic correction of the *C9ORF72* HRE.

Finally, other major neuropathological hallmarks of C9-FTD/ALS such as p62 inclusions co-localising with DPRs or TDP-43 cytoplasmic mislocalisation and aggregation are not a common finding in *C9ORF72* iPSC models. Some iPSC studies have shown evidence for elevated p62 levels (Almeida et al., 2013; Dafinca et al., 2016), and p62 cytoplasmic inclusions have been observed under basal conditions (Dafinca et al., 2016) and upon chronic sodium arsenite stress (Ratti et al., 2020), however, p62 pathology is not a common finding among iPSC studies. Importantly, even though a nucleocytoplasmic shift of TDP-43 has been reported in iPSC studies (Yuva-Aydemir et al., 2019; Zhang et al., 2015), the typical cytoplasmic TDP-43 inclusion pathology in C9-FTD/ALS has not been yet recapitulated in vitro by iPSC studies under basal conditions. However, it was recently shown that chronic, mild oxidative stress insult by sodium arsenite treatment was able to induce the recruitment of TDP-43 into stress granules as well as the formation of distinct cytoplasmic aggregates of phosphorylated TDP-43 in *C9ORF72* iPSC-MNs (Ratti et al., 2020).

Together, these studies show that iPSC-neurons from patients with the *C9ORF72* HRE can recapitulate RNA foci, DPRs and *C9ORF72* haploinsufficiency.

5.2. Investigating C9ORF72 function in iPSC-neurons

A role of C9ORF72 protein in endosomal trafficking and autophagy has been suggested (Farg et al., 2014) and several independent studies have further supported the function of C9ORF72 in the induction of autophagy (Webster et al., 2016; Sellier et al., 2016; Sullivan et al., 2016; Yang et al., 2016). C9ORF72 iPSC studies have confirmed the role of C9ORF72 protein in autophagy and elucidated novel aspects of C9ORF72 cellular function. *C9ORF72* patient-derived neurons were found to exhibit elevated levels of the autophagy marker p62 compared to controls (Almeida et al., 2013; Dafinca et al., 2016) reminiscent of the p62 positive/ubiquitin positive/TDP43 negative DPR pathology observed in C9-FTD/ALS patients (Mackenzie et al., 2014). Compromised autophagy and a reduction in basal autophagy levels have been observed in *C9ORF72* iPSC-neurons (Webster et al., 2016; Almeida et al., 2013). Compromised extracellular vesicle secretion and endosome formation as well as dysfunctional trans-Golgi network were also observed in *C9ORF72* HRE MNs by Aoki et al. (Aoki et al., 2017). The C9ORF72 protein was found to localise in early endosomes and was required for normal vesicle trafficking and lysosomal biogenesis in iPSC-MNs (Shi et al., 2018). C9ORF72 haploinsufficiency could therefore trigger neurodegeneration by causing accumulation of glutamate receptors, leading to MN excitotoxicity, and hypersensitivity of MNs to neurotoxic DPRs by impairing their clearance (Shi et al., 2018). This could be rescued by restoring C9ORF72 levels or treatment with small molecule modulators of vesicle trafficking. Finally, Sivadasan et al. provided evidence that C9ORF72 regulates axonal actin dynamics via regulation of the GTPase activity of Arf6 and the phosphorylation of cofilin, a ubiquitous actin-binding factor required for the reorganization of actin filaments (Sivadasan et al., 2016).

5.3. Novel pathways identified in C9ORF72 iPSC-neurons

Importantly, apart from recapitulating C9-FTD/ALS pathology, a plethora of iPSC studies have shed light on novel disease mechanisms linked to *C9ORF72* HRE. Nucleocytoplasmic transport has been found by several independent groups to be impaired in FTD/ALS linked to *C9ORF72* HRE (Zhang et al., 2015; Freibaum et al., 2015; Jovicic et al., 2015; Cheng et al., 2019; Moore et al., 2019). A disrupted nuclear-cytoplasmic pattern for total RNA (Freibaum et al., 2015), Ran GTPase-activating protein 1 (RanGAP1) (Zhang et al., 2015; Cheng et al., 2019), TDP-43 (Zhang et al., 2015), Ran-GEF RCC1 (Jovicic et al., 2015), and RNA editing enzyme adenosine deaminase acting on RNA 2 (ADAR2) (Moore et al., 2019) have been identified in *C9ORF72* HRE neurons.

Several studies have investigated dysregulated cellular processes leading to increased vulnerability *C9ORF72* iPSC-neurons to ER and oxidative stress, mitochondrial dysfunction and excitotoxicity (Dafinca et al., 2016; Donnelly et al., 2013; Lopez-Gonzalez et al., 2016; Selvaraj et al., 2018; Shi et al., 2018; Andrade et al., 2020). Dafinca et al. reported elevated ER calcium levels, reduced mitochondrial membrane potential and reduced levels of the antiapoptotic protein Bcl-2 in *C9ORF72* patient-derived MNs compared to control MNs (Dafinca et al.,

2016). Furthermore, *C9ORF72* HRE cortical and MNs displayed increased susceptibility to apoptosis, elevated p62 levels, abnormal protein aggregation and stress granule formation compared to control neurons. In a follow-up study, Ababneh et al. reported reversal of all HRE-related phenotypes upon CRISPR/Cas9 correction of the HRE in iPSC lines from one patient (Ababneh et al., 2020). The phenotypes included susceptibility of *C9ORF72* MNs to apoptosis, increased number of stress granules, HRE-containing intron 1 retention, 5′ CpG hypermethylation and reduced *C9ORF72* RNA expression. Several other studies have also shown vulnerability of *C9ORF72* patient-derived neurons to excitotoxicity (Donnelly et al., 2013; Selvaraj et al., 2018; Shi et al., 2018). Lopez-Gonzalez et al. demonstrated that poly-GR led to mitochondrial dysfunction, age-dependent increase in oxidative stress and DNA damage as indicated by an increase in DNA damage marker γH2AX, in *C9ORF72* patient-derived MNs (Lopez-Gonzalez et al., 2016). They also showed that reduction of oxidative stress partially reduced DNA damage in *C9ORF72* patient-derived MNs suggesting that oxidative stress could play an important role in the disease pathogenesis and its reduction has therapeutic potential in C9-FTD/ALS. Additional studies have further implicated the DNA damage response in C9ORF72 neurodegeneration. Increased DNA damage marker γH2AX as well as RAD5, a component of the SSA repair machinery, and phosphorylated RAD52, were found in *C9ORF72* patient-derived MNs (Andrade et al., 2020). CRISPR/Cas-9-mediated excision of the HRE resulted in reduction of RAD52 hyperactivation. These findings suggest HRE-mediated DNA damage in patient-derived MNs leads to deficits in homology-directed DNA double strand break (DSB) repair pathways.

Altered axonal trafficking, axonal degeneration and synaptic vesicle recycling have also been observed in *C9ORF72* patient-derived neurons (Yuva-Aydemir et al., 2019; Abo-Rady et al., 2020; Coyne et al., 2017). Coyne et al. showed that synaptic vesicle cycling was impaired in *C9ORF72* patient-derived MNs due to posttranscriptional reduction in the levels of the Hsc70-4/HSPA8 chaperone (Coyne et al., 2017). Axonal degeneration and partial TDP-43 translocation to the cytoplasm, reminiscent of the TDP-43 pathology observed in C9-FTD/ALS patients, was observed in *C9ORF72* patient-derived neurons (Yuva-Aydemir et al., 2019). The authors demonstrated that transcription elongation factor AFF2/FMR2 regulates the transcription of the HRE and CRISPR-Cas9-mediated knockout of AFF2/FMR2 resulted in decreased expression of the mutant *C9ORF72* allele containing the HRE and rescue of axonal degeneration and TDP-43 mislocalisation. Finally, patient-derived MNs exhibited axonal transport defects, as indicated by lysosomal track displacement in distal and proximal axons, compared to control MNs (Abo-Rady et al., 2020). This was accompanied by reduced levels of ubiquitously expressed chaperone HSP70 and altered stress granule formation compared to control MNs. Interestingly, all these phenotypes were exacerbated in isogenic *C9ORF72* patient-derived MNs that contained the HRE as well as a *C9ORF72* knockout, supporting a combination of gain and loss of function mechanisms in C9-ALS/FTD pathogenesis.

Finally, the first *C9ORF72* three dimensional neuronal model revealed re-engagement of cell cycle-associated proteins and a senescence-associated secretory phenotype in *C9ORF72* patient-derived neurons (Porterfield et al., 2020). Specifically, *C9ORF72* patient-derived neurons grown on Alvetex scaffold spontaneously re-expressed cyclin D1 12 weeks post-differentiation, suggesting cell cycle re-engagement. *C9ORF72* neurons exhibited increased expression of senescence-associated genes including CXCL8, a chemokine overexpressed by senescent cells. In addition to this, increased levels of components of the senescence-associated secretory phenotype were present in media from *C9ORF72* neurons compared to controls.

5.4. Alterations in neuronal function in C9ORF72 iPSC-neurons

Neuronal excitability impairments are frequently observed in *C9ORF72* patients (Williams et al., 2013), therefore several studies have investigated the electrophysiological properties of *C9ORF72* iPSC-neurons. Two studies have found that *C9ORF72* patient-derived MNs were characterised by hyperexcitability compared to control MNs at 2 to 4 weeks post differentiation (Devlin et al., 2015; Wainger et al., 2014). In direct contrast, Sareen et al. reported loss of excitability in 2-month-old *C9ORF72* patient-derived MNs as well as altered expression of genes involved in membrane excitability, including the delayed rectifier potassium channel (KCNQ3) which is consistent with hypoexcitability (Sareen et al., 2013). These conflicting findings between the studies may be attributed to the different developmental stage of the MNs, as indicated by a temporal analysis of *C9ORF72* patient-derived MN excitability (Devlin et al., 2015). Devlin et al. showed that *C9ORF72* patient-derived MNs were characterised by intrinsic hyperexcitability at early time points (3–4 weeks) in culture, followed by progressive loss of action potential output and synaptic activity in MNs reaching 9–10 weeks in culture. Interestingly, the loss of excitability manifests at a similar timepoint during MN differentiation as in the study of Sareen et al. (Sareen et al., 2013). Finally, Selvaraj et al. showed no differences in the excitability of *C9ORF72* patient-derived MNs compared to control MNs and isogenic CRISPR/Cas9 *C9ORF72* HRE-corrected MNs (Selvaraj et al., 2018). The authors attributed the lack of changes in excitability to the purity of MN cultures, compared to other studies using mixed cultures of MNs and glia, suggesting glia-mediated non-cell-autonomous mechanisms may alter MN function. Indeed, in a follow-up study, Zhao et al. demonstrated that *C9ORF72* patient-derived astrocytes induced progressive loss of action potential output in control iPSC-MNs caused by an underlying loss of voltage activated Na + and K+ currents (Zhao et al., 2020).

5.5. Non-cell-autonomous disease mechanisms in C9ORF72 iPSC-neurons

Patient-derived iPSC models provide an ideal platform to investigate non-cell-autonomous disease mechanisms. To date, several groups have demonstrated a toxic effect of *C9ORF72* patient-derived astrocytes and oligodendrocytes to MNs or other cell types either in co-cultures or via conditioned media. In an early study of non-cell-autonomous toxicity mechanisms in C9-ALS, Meyer et al. showed that *C9ORF72* transdifferentiated human astrocytes were toxic to co-cultured mouse MNs (Meyer et al., 2014). *C9ORF72* iPSC-astrocytes were shown to modulate the autophagy pathway in a non-cell-autonomous manner (Madill et al., 2017). Specifically, cells treated with patient-derived astrocyte conditioned medium exhibited reduced expression of the autophagosomal marker LC3-II, with a concomitant accumulation of p62 puncta and increased SOD1 expression. Increased oxidative stress was detected in *C9ORF72* patient-derived astrocytes and *C9ORF72* astrocyte conditioned media was also found to be neurotoxic by inducing oxidative stress in control MNs (Birger et al., 2019). Varcianna et al. reported dysregulation of extracellular vesicle formation and miRNA cargo in *C9ORF72* induced astrocytes which affected neurite network maintenance and MN survival (Varcianna et al., 2019). They identified downregulation of miR-494-3p, a negative regulator of the axon guidance protein semaphorin 3A (SEMA3A), and showed that restoration of miR-494-3p levels can downregulate Sema3A levels in MNs and increase MN survival. *C9ORF72* patient-derived astrocytes recapitulated key pathological features of C9-ALS and caused a progressive loss of action potential output in co-cultured control MNs which was reversed upon CRISPR/Cas-9-mediated excision of the HRE (Zhao et al., 2020). Importantly, these phenotypes were only present in control MNs co-cultured with *C9ORF72* patient-derived astrocytes and not in *C9ORF72* patient-derived MN-enriched cultures alone, providing further evidence for the role of non-cell-autonomous toxicity mechanisms in neurodegeneration. Finally, apart from astrocytes, patient-derived oligodendrocytes have also been shown to induce MN death in both co-cultures and via oligodendrocyte conditioned media (Ferraiuolo et al., 2016).

5.6. Using C9ORF72 iPSC models for the development of novel therapeutics

Ultimately, the use of iPSCs for the study of *C9ORF72* FTD/ALS pathogenic mechanisms is aimed at the development of novel therapies. Two independent studies have provided evidence for the therapeutic potential of antisense oligonucleotides (ASOs) in C9-FTD/ALS which are currently being tested in *C9ORF72* HRE patients (https://clinicaltrials.gov/ct2/show/study/NCT03626012) (Sareen et al., 2013; Donnelly et al., 2013). Donnelly et al. reported sequestration of RNA editing regulator ADARB2 by the *C9ORF72* HRE expanded RNA, aberrant gene expression and susceptibility to glutamate excitotoxicity in *C9ORF72* HRE mixed neurons compared to controls (Donnelly et al., 2013). In the second ASO study by Sareen et al. the *C9ORF72* patient-derived MNs exhibited RNA foci that co-localised with RNA-binding proteins hnRNPA1 and Pur-α, as well as aberrant gene expression, and reduced excitability compared to control MNs (Sareen et al., 2013). In both studies the use of ASOs targeting the *C9ORF72* transcript resulted in reversal of the toxicity phenotypes in patient-derived neurons. Furthermore, as the ASO-mediated *C9ORF72* knockdown had no adverse effect on patient-derived neurons, the authors argued against a loss of function mechanism as the major pathogenic cause of C9-FTD/ALS. However, recent studies have elucidated the important function of C9ORF72 in autophagy and provided evidence for a contribution of *C9ORF72* haploinsufficiency in FTD/ALS pathogenesis, proposing the use of ASOs that do not reduce *C9ORF72* expression. Interestingly, the use of ASOs restored the impaired nucleocytoplasmic transport phenotype that was responsible for the abnormal nuclear/cytoplasmic ratios of Ran and TDP-43 in another study of *C9ORF72* HRE neurons (Zhang et al., 2015). Collectively, the ASO intervention studies in human *C9ORF72* iPSC neurons have shown that specific targeting of the *C9ORF72* transcript can rescue gain of function toxicity and has therapeutic value. Using small molecules that bind and specifically stabilise the *C9ORF72* HRE G-quadruplex RNA, Simone et al. demonstrated a reduction in RNA foci burden in both *C9ORF72* HRE cortical neurons and MNs as well as a reduction in the levels of poly-GP in *C9ORF72* HRE MNs (Simone et al., 2018). These data provide proof of principle that targeting the *C9ORF72* HRE G-quadruplex structure has therapeutic potential. Finally, in a phenotypic screen to repurpose existing drugs, Imamura et al. identified the Src/c-Abl pathway as a novel potential therapeutic target in ALS, and Bosutinib, a Src/c-Abl inhibitor, was shown to increase survival of *C9ORF72* patient-derived MNs (Imamura et al., 2017).

6. iPSC models of *TARDBP* mutations

Bilican et al. differentiated clonal iPSC lines from two controls and an ALS patient with a *TARDBP* M337V mutation into MNs (Bilican et al., 2012). They noted higher levels of soluble and detergent-resistant TDP-43 in M337V MNs, despite apparently normal levels of nuclear TDP-43. They found higher levels of C-terminal TDP-43 fragments in the insoluble fraction and higher levels of full-length TDP-43 in the soluble fraction. M337V MNs had reduced cell viability and an increased sensitivity to a PI3K inhibitor (LY294002), although no differences in the response to a MAPK inhibitor (U0126) or an endoplasmic reticulum stressor (tunicamycin) were observed. The same iPSC lines were used by Serio et al. to generate astrocytes (Serio et al., 2013). The astrocytes had similar phenotypes to the MNs including mislocalised, cytoplasmic TDP-43, increased levels of soluble TDP-43 and reduced viability. The authors suggested that the increased TDP-43 levels are likely due to the mutation resulting in PTMs that increase TDP-43 stability and/or slow its clearance. In contrast to the MNs, they found no difference in detergent-resistant, insoluble TDP-43, indicating that the mutation has distinct cell type specific effects. Co-culture of MNs with either control or M337V astrocytes resulted in improved viability, showing that M337V astrocytes do not exert a toxic effect on MNs, unlike what has previously been observed in SOD1-linked ALS (Nagai et al., 2007).

Zhang et al. differentiated iPSC lines from an FTD/ALS patient with *TARDBP* A90V mutation, an unaffected family member with no known disease-causing mutations, and the M337V iPSC line previously used in the Bilican et al. study into neurons (Zhang et al., 2013; Bilican et al., 2012). Treatment with the broad-spectrum kinase inhibitor staurosporine resulted in cytoplasmic mislocalisation of TDP-43 in both control and patient lines, but with a higher ratio of cytoplasmic: nuclear TDP-43, lower levels of total TDP-43 and higher rates of neuronal death in the patient neurons. They also identified decreased levels of the neuroprotective miR-9 and its precursor (miR-9-2) in the patient-derived neurons. They did not find differences in TDP-43 profile between the control and patient iPSC-neurons under control conditions or in response to other stressors. Bossolasco et al. also did not find any significant increase in cytoplasmically mislocalised TDP-43 in neurons with the A382T mutation (Bossolasco et al., 2018) under control conditions.

Multiple studies have also shown the potential of iPSCs from patients with *TARDBP* mutations as a suitable model for drug screening. Egawa et al. found cytoplasmically mislocalised, aggregated TDP-43 and shorter neurites in iPSC-MNs from ALS patients with *TARDBP* (Q343R/M337 V/G298S) mutations (Egawa et al., 2012). It is not clear if this identification of aggregates, which were either not detected or not mentioned in the previous studies using iPSCs with M337V mutations, was due to differentiation to a particular cell-type or differences in detection methods. Ratti et al. did find stress granules and phosphorylated TDP-43 aggregates in *TARDBP* iPSC-MNs after inducing stress through sodium arsenite treatment, whereas there were only very low levels of phosphorylated TDP-43 under control conditions (Ratti et al., 2020). This suggests that stress might be necessary to induce TDP-43 pathology in iPSC-derived neurons and might explain differences in TDP-43 observations between studies. In the patients MNs, Egawa et al. found the spliceosomal factor SNRPB2 bound to TDP-43, which could be rescued by the histone acetyltransferase inhibitor, anacardic acid. Another study found abnormalities in mitochondria, lysosomes and axonal trafficking in G294V neurons, the latter was rescued by treating with the osmolyte D-sorbitol (Kreiter et al., 2018). Burkhardt et al. developed a screen using iPSC-MNs from sporadic and familial ALS patients, including a patient with a *TARDBP* mutation and found hyper-phosphorylated TDP-43 aggregates in neurons from the sporadic ALS patients but did not detect aggregates in control neurons or neurons from the *TARDBP* A315T patient. They identified compounds that reduced TDP-43 aggregation in patient neurons. They also detected higher levels of TDP-43 in MNs but did not find higher levels in the sporadic ALS neurons with aggregates (Burkhardt et al., 2013). Yang et al. used iPSC-neurons further validate the treatment potential of Kenpaullone, a multikinase inhibitor that had been found to increase neuronal survival in mutant *SOD1* mouse embryonic stem cells (Yang et al., 2013). Together, these studies show that iPSC-neurons with mutations in *TARDBP* can recapitulate key aspects of TDP-43 pathology (Fig. 5), although they may not display all of the phenotypes seen in *TARDBP* mutation patients, and that they can be used to identify or validate promising treatment options.

7. Summary and future directions

The generation of iPSCs from patients with phenotypes/genotypes of interest and their subsequent differentiation into homogenous populations of specific cell types has enabled the development of patient-specific in vitro models of familial FTD (Fig. 1). This approach has been successfully used in an ever-increasing number of studies to model the most common genetic causes of FTD and FTD-ALS. In spite of this early success, several challenges still remain. The advantages and limitations of using iPSC-derived cells to model FTD have been summarised in Table 5.

On a technical level, the cost of iPSC work can be prohibitive, and

restricts the number of patient and control lines that can be used in a single study. Although iPSC-neurons do present with some key markers of FTD, for example increased tau phosphorylation and tau mislocalisation in FTD with *MAPT* mutations (Fig. 2), progranulin haploinsufficiency in FTD with *GRN* mutations (Fig. 3) and TDP-43 mislocalisation in FTD with *GRN* or *TARDBP* mutations (Figs. 3 and 5), these models do not recapitulate the full pathologies observed in FTD patients. For example, iPSC- neurons with *MAPT* mutations, do not show neurofibrillary tangles, only occasional accumulations of insoluble phosphorylated or misfolded tau species (Iovino et al., 2015; Imamura et al., 2016b) and studies using iPSC-neurons with *GRN* and *TARDBP* mutations do not always find TDP-43 aggregation, mislocalisation or increased levels of insoluble TDP-43 (Tables 2 and 4). Similarly, although *C9ORF72* iPSC studies have successfully recapitulated C9-FTD/ALS pathology associated with RNA foci and DPRs, they do not develop robust TDP-43 pathology, only early-stage TDP-43 mislocalisation, unless chronic stress is applied in neuronal cultures (Ratti et al., 2020). Multiple transcriptomics studies have demonstrated that iPSC-neurons are fetal in nature (Patani et al., 2012; Handel et al., 2016), which presents a challenge when investigating age-related neurodegenerative diseases such as FTD. Induction of age-associated phenotypes to increase the physiological relevance of iPSC-derived models could be explored, for example, introducing reactive oxidative stress, DNA damage and mitochondrial damage, traits typically associated with aged cells (Guillaumet-Adkins et al., 2017). Telomerase inhibitors (Vera et al., 2016) and progerin, a derivative of lamin A associated with premature aging (Miller et al., 2013) have been used to induce age-associated phenotypes, such as accumulation of ROS and DNA damage and shorter dendrites in iPSC-neurons.

Inter and intra-patient variability in iPSCs, linked to genetic heterogeneity, is a known challenge of working with human iPSCs (Kilpinen et al., 2017), and the generation of isogenic controls by gene-editing may help to control this issue (Preza et al., 2016). However, understanding the contribution of gene modifiers to cellular phenotypes is an important question: for example, *TMEM106B* variants can modify the phenotype of both *GRN* and *C9ORF72* mutation carriers (Finch et al., 2011; van Blitterswijk et al., 2014; Gallagher et al., 2014) and the protective variant has been shown to ameliorate lysosomal phenotypes in vitro (Klein et al., 2017). Most studies discussed here did not mention the *TMEM106B* genotype of the cell lines used. Further, the genetic and neuropathological overlap between FTD and ALS due to *C9ORF72* repeat expansions and TDP-43 pathology respectively, means that most studies have used either cortical or MNs, and we must exercise caution when extrapolating results from one to other. Future studies to examine neuronal subtype-specific effects, in cells from deeply-phenotyped patients with either ALS or FTD will help us understand the selective vulnerability of these cell types. It should be noted that the majority of studies have generated and analysed only one iPSC-derived neural cell type, such as neurons. It will again be important to understand the contribution of astrocytes and microglia to FTD, and the cross-talk between these cell types in complex, co-culture models. Increased optimisation of 3D cell culture, whereby astrocytes and microglia are infused into neuronal organoids may help us explore cellular crosstalk in FTD (Park et al., 2018). However, using organoids to model neurodegeneration comes with its own merits and limitations. Whilst organoids are advantageous in that they better replicate the complex structural architecture of the brain compared to 2D models, a lack of tissue maturity and vascularisation limit their usefulness (Grenier et al., 2020). To date, the majority of research using organoids to model neurodegeneration has been focused on Alzheimer's disease (Park et al., 2018; Lee et al., 2016; Raja et al., 2016), however it will be interesting to see how 3D models are used to research FTD and ALS as organoid protocols and molecular techniques continue to improve.

In spite of the aforementioned challenges, iPSC models have given unique insights into disease mechanisms of *MAPT*, *GRN*, *C9ORF72* and *TARDBP* mutations, and provide a novel, physiologically relevant model for drug screening. As future work addresses the challenges outlined above, these patient-derived models will continue to give us unique insights into the molecular mechanisms underpinning neurodegeneration in FTD.

Acknowledgements

EP and SW are supported by the National Institute for Health Research University College London Hospitals Biomedical Research Centre. SW is supported by an Alzheimer's Research UK Senior Research Fellowship (ARUK-SRF2016B-2).GL is supported by a BBSRC CASE studentship and JC is supported by the EPSRC. We apologise to colleagues whose work has been omitted due to space constraints.

References

Ababneh, N.A., Scaber, J., Flynn, R., Douglas, A., Barbagallo, P., Candalija, A., et al., 2020. Correction of amyotrophic lateral sclerosis related phenotypes in induced pluripotent stem cell-derived motor neurons carrying a hexanucleotide expansion mutation in C9orf72 by CRISPR/Cas9 genome editing using homology-directed repair. Hum. Mol. Genet. 29 (13), 2200–2217.

Abo-Rady, M., Kalmbach, N., Pal, A., Schludi, C., Janosch, A., Richter, T., et al., 2020. Knocking out C9ORF72 exacerbates axonal trafficking defects associated with hexanucleotide repeat expansion and reduces levels of heat shock proteins. Stem Cell Reports. 14 (3), 390–405.

Ahmed, Z., Sheng, H., Xu, Y.F., Lin, W.L., Innes, A.E., Gass, J., et al., 2010. Accelerated lipofuscinosis and ubiquitination in granulin knockout mice suggest a role for progranulin in successful aging. Am. J. Pathol. 177 (1), 311–324.

Almeida, S., Zhang, Z., Coppola, G., Mao, W., Futai, K., Karydas, A., et al., 2012. Induced pluripotent stem cell models of progranulin-deficient frontotemporal dementia uncover specific reversible neuronal defects. Cell Rep. 2 (4), 789–798.

Almeida, S., Gascon, E., Tran, H., Chou, H.J., Gendron, T.F., Degroot, S., et al., 2013. Modeling key pathological features of frontotemporal dementia with C9ORF72 repeat expansion in iPSC-derived human neurons. Acta Neuropathol. 126 (3), 385–399.

Almeida MR, Macario MC, Ramos L, Baldeiras I, Ribeiro MH, Santana I. Portuguese family with the co-occurrence of frontotemporal lobar degeneration and neuronal ceroid lipofuscinosis phenotypes due to progranulin gene mutation. Neurobiol Aging. 2016a;41:200 e1-e5.

Almeida, S., Gao, F., Coppola, G., Gao, F.B., 2016b. Suberoylanilide hydroxamic acid increases progranulin production in iPSC-derived cortical neurons of frontotemporal dementia patients. Neurobiol. Aging 42, 35–40.

Alonso Adel, C., Mederlyova, A., Novak, M., Grundke-Iqbal, I., Iqbal, K., 2004. Promotion of hyperphosphorylation by frontotemporal dementia tau mutations. J. Biol. Chem. 279 (33), 34873–34881.

Amador-Ortiz, C., Lin, W.L., Ahmed, Z., Personett, D., Davies, P., Duara, R., et al., 2007. TDP-43 immunoreactivity in hippocampal sclerosis and Alzheimer's disease. Ann. Neurol. 61 (5), 435–445.

Amick, J., Roczniak-Ferguson, A., Ferguson, S.M., 2016. C9orf72 binds SMCR8, localizes to lysosomes, and regulates mTORC1 signaling. Mol. Biol. Cell 27 (20), 3040–3051.

Andrade, N.S., Ramic, M., Esanov, R., Liu, W., Rybin, M.J., Gaidosh, G., et al., 2020. Dipeptide repeat proteins inhibit homology-directed DNA double strand break repair in C9ORF72 ALS/FTD. Mol. Neurodegener. 15 (1), 13.

Andreadis, A., Broderick, J.A., Kosik, K.S., 1995. Relative exon affinities and suboptimal splice site signals lead to non-equivalence of two cassette exons. Nucleic Acids Res. 23 (17), 3585–3593.

Aoki, Y., Manzano, R., Lee, Y., Dafinca, R., Aoki, M., Douglas, A.G.L., et al., 2017. C9orf72 and RAB7L1 regulate vesicle trafficking in amyotrophic lateral sclerosis and frontotemporal dementia. Brain. 140 (4), 887–897.

Arai, T., Hasegawa, M., Akiyama, H., Ikeda, K., Nonaka, T., Mori, H., et al., 2006. TDP-43 is a component of ubiquitin-positive tau-negative inclusions in frontotemporal lobar degeneration and amyotrophic lateral sclerosis. Biochem. Biophys. Res. Commun. 351 (3), 602–611.

Arrant, A.E., Nicholson, A.M., Zhou, X., Rademakers, R., Roberson, E.D., 2018. Partial Tmem106b reduction does not correct abnormalities due to progranulin haploinsufficiency. Mol. Neurodegener. 13 (1), 32.

Ash, P.E., Bieniek, K.F., Gendron, T.F., Caulfield, T., Lin, W.L., Dejesus-Hernandez, M., et al., 2013. Unconventional translation of C9ORF72 GGGGCC expansion generates insoluble polypeptides specific to c9FTD/ALS. Neuron. 77 (4), 639–646.

Ayala, Y.M., Zago, P., D'Ambrogio, A., Xu, Y.F., Petrucelli, L., Buratti, E., et al., 2008. Structural determinants of the cellular localization and shuttling of TDP-43. J. Cell Sci. 121 (Pt 22), 3778–3785.

Baborie, A., Griffiths, T.D., Jaros, E., McKeith, I.G., Burn, D.J., Richardson, A., et al., 2011. Pathological correlates of frontotemporal lobar degeneration in the elderly. Acta Neuropathol. 121 (3), 365–371.

Baker, M., Litvan, I., Houlden, H., Adamson, J., Dickson, D., Perez-Tur, J., et al., 1999. Association of an extended haplotype in the tau gene with progressive supranuclear palsy. Hum. Mol. Genet. 8 (4), 711–715.

Baker, M., Mackenzie, I.R., Pickering-Brown, S.M., Gass, J., Rademakers, R., Lindholm, C., et al., 2006. Mutations in progranulin cause tau-negative frontotemporal dementia linked to chromosome 17. Nature. 442 (7105), 916–919.

Bardelli, D., Sassone, F., Colombrita, C., Volpe, C., Gumina, V., Peverelli, S., et al., 2020.

Reprogramming fibroblasts and peripheral blood cells from a C9ORF72 patient: a proof-of-principle study. J. Cell. Mol. Med. 24 (7), 4051–4060.
Beel, S., Moisse, M., Damme, M., De Muynck, L., Robberecht, W., Van Den Bosch, L., et al., 2017. Progranulin functions as a cathepsin D chaperone to stimulate axonal outgrowth in vivo. Hum. Mol. Genet. 26 (15), 2850–2863.
Beevers, J.E., Lai, M.C., Collins, E., Booth, H.D.E., Zambon, F., Parkkinen, L., et al., 2017. MAPT genetic variation and neuronal maturity Alter isoform expression affecting axonal transport in iPSC-derived dopamine neurons. Stem Cell Reports. 9 (2), 587–599.
Belzil, V.V., Bauer, P.O., Gendron, T.F., Murray, M.E., Dickson, D., Petrucelli, L., 2014. Characterization of DNA hypermethylation in the cerebellum of c9FTD/ALS patients. Brain Res. 1584, 15–21.
Berg, L., McKeel Jr., D.W., Miller, J.P., Storandt, M., Rubin, E.H., Morris, J.C., et al., 1998. Clinicopathologic studies in cognitively healthy aging and Alzheimer's disease: relation of histologic markers to dementia severity, age, sex, and apolipoprotein E genotype. Arch. Neurol. 55 (3), 326–335.
Bilican, B., Serio, A., Barmada, S.J., Nishimura, A.L., Sullivan, G.J., Carrasco, M., et al., 2012. Mutant induced pluripotent stem cell lines recapitulate aspects of TDP-43 proteinopathies and reveal cell-specific vulnerability. Proc. Natl. Acad. Sci. U. S. A. 109 (15), 5803–5808.
Birger, A., Ben-Dor, I., Ottolenghi, M., Turetsky, T., Gil, Y., Sweetat, S., et al., 2019. Human iPSC-derived astrocytes from ALS patients with mutated C9ORF72 show increased oxidative stress and neurotoxicity. EBioMedicine. 50, 274–289.
Biswas, M.H.U., Almeida, S., Lopez-Gonzalez, R., Mao, W., Zhang, Z., Karydas, A., et al., 2016. MMP-9 and MMP-2 contribute to neuronal cell death in iPSC models of frontotemporal dementia with MAPT mutations. Stem Cell Reports. 7 (3), 316–324.
Borroni, B., Bonvicini, C., Alberici, A., Buratti, E., Agosti, C., Archetti, S., et al., 2009. Mutation within TARDBP leads to frontotemporal dementia without motor neuron disease. Hum. Mutat. 30 (11), E974–E983.
Borroni, B., Archetti, S., Del Bo, R., Papetti, A., Buratti, E., Bonvicini, C., et al., 2010. TARDBP mutations in frontotemporal lobar degeneration: frequency, clinical features, and disease course. Rejuvenation Res. 13 (5), 509–517.
Bossolasco, P., Sassone, F., Gumina, V., Peverelli, S., Garzo, M., Silani, V., 2018. Motor neuron differentiation of iPSCs obtained from peripheral blood of a mutant TARDBP ALS patient. Stem Cell Res. 30, 61–68.
Bott, N.T., Radke, A., Stephens, M.L., Kramer, J.H., 2014. Frontotemporal dementia: diagnosis, deficits and management. Neurodegener Dis Manag. 4 (6), 439–454.
Braak, H., Braak, E., 1991. Neuropathological stageing of Alzheimer-related changes. Acta Neuropathol. 82 (4), 239–259.
Buratti, E., 2018. TDP-43 post-translational modifications in health and disease. Expert Opin. Ther. Targets 22 (3), 279–293.
Burkhardt, M.F., Martinez, F.J., Wright, S., Ramos, C., Volfson, D., Mason, M., et al., 2013. A cellular model for sporadic ALS using patient-derived induced pluripotent stem cells. Mol. Cell. Neurosci. 56, 355–364.
Butler, V.J., Cortopassi, W.A., Argouarch, A.R., Ivry, S.L., Craik, C.S., Jacobson, M.P., et al., 2019. Progranulin stimulates the in vitro maturation of pro-cathepsin D at acidic pH. J. Mol. Biol. 431 (5), 1038–1047.
Caffrey, T.M., Joachim, C., Wade-Martins, R., 2008. Haplotype-specific expression of the N-terminal exons 2 and 3 at the human MAPT locus. Neurobiol. Aging 29 (12), 1923–1929.
Cairns, N.J., Neumann, M., Bigio, E.H., Holm, I.E., Troost, D., Hatanpaa, K.J., et al., 2007. TDP-43 in familial and sporadic frontotemporal lobar degeneration with ubiquitin inclusions. Am. J. Pathol. 171 (1), 227–240.
Canafoglia, L., Morbin, M., Scaioli, V., Pareyson, D., D'Incerti, L., Fugnanesi, V., et al., 2014. Recurrent generalized seizures, visual loss, and palinopsia as phenotypic features of neuronal ceroid lipofuscinosis due to progranulin gene mutation. Epilepsia. 55 (6), e56–e59.
Chang, M.C., Srinivasan, K., Friedman, B.A., Suto, E., Modrusan, Z., Lee, W.P., et al., 2017. Progranulin deficiency causes impairment of autophagy and TDP-43 accumulation. J. Exp. Med. 214 (9), 2611–2628.
Cheng, W., Wang, S., Zhang, Z., Morgens, D.W., Hayes, L.R., Lee, S., et al., 2019. CRISPR-Cas9 screens identify the RNA helicase DDX3X as a repressor of C9ORF72 (GGGGCC) n repeat-associated non-AUG translation. Neuron. 104 (5), 885–898 (e8).
Choi, S.H., Kim, Y.H., Hebisch, M., Sliwinski, C., Lee, S., D'Avanzo, C., et al., 2014. A three-dimensional human neural cell culture model of Alzheimer's disease. Nature. 515 (7526), 274–278.
Chow, T.W., Miller, B.L., Hayashi, V.N., Geschwind, D.H., 1999. Inheritance of frontotemporal dementia. Arch. Neurol. 56 (7), 817–822.
Clark, L.N., Poorkaj, P., Wszolek, Z., Geschwind, D.H., Nasreddine, Z.S., Miller, B., et al., 1998. Pathogenic implications of mutations in the tau gene in pallido-ponto-nigral degeneration and related neurodegenerative disorders linked to chromosome 17. Proc. Natl. Acad. Sci. U. S. A. 95 (22), 13103–13107.
Cohen, T.J., Hwang, A.W., Restrepo, C.R., Yuan, C.X., Trojanowski, J.Q., Lee, V.M., 2015. An acetylation switch controls TDP-43 function and aggregation propensity. Nat. Commun. 6, 5845.
Cohen-Hadad, Y., Altarescu, G., Eldar-Geva, T., Levi-Lahad, E., Zhang, M., Rogaeva, E., et al., 2016. Marked differences in C9orf72 methylation status and isoform expression between C9/ALS human embryonic and induced pluripotent stem cells. Stem Cell Reports. 7 (5), 927–940.
Conrad, C., Andreadis, A., Trojanowski, J.Q., Dickson, D.W., Kang, D., Chen, X., et al., 1997. Genetic evidence for the involvement of tau in progressive supranuclear palsy. Ann. Neurol. 41 (2), 277–281.
Coppola, G., Chinnathambi, S., Lee, J.J., Dombroski, B.A., Baker, M.C., Soto-Ortolaza, A.I., et al., 2012. Evidence for a role of the rare p.A152T variant in MAPT in increasing the risk for FTD-spectrum and Alzheimer's diseases. Hum. Mol. Genet. 21 (15), 3500–3512.
Coyne, A.N., Lorenzini, I., Chou, C.C., Torvund, M., Rogers, R.S., Starr, A., et al., 2017. Post-transcriptional inhibition of Hsc70-4/HSPA8 expression leads to synaptic vesicle cycling defects in multiple models of ALS. Cell Rep. 21 (1), 110–125.
Cruts, M., Gijselinck, I., van der Zee, J., Engelborghs, S., Wils, H., Pirici, D., et al., 2006. Null mutations in progranulin cause ubiquitin-positive frontotemporal dementia linked to chromosome 17q21. Nature. 442 (7105), 920–924.
Dafinca, R., Scaber, J., Ababneh, N., Lalic, T., Weir, G., Christian, H., et al., 2016. C9orf72 hexanucleotide expansions are associated with altered endoplasmic reticulum calcium homeostasis and stress granule formation in induced pluripotent stem cell-derived neurons from patients with amyotrophic lateral sclerosis and frontotemporal dementia. Stem Cells 34 (8), 2063–2078.
Dardis, A., Zampieri, S., Canterini, S., Newell, K.L., Stuani, C., Murrell, J.R., et al., 2016. Altered localization and functionality of TAR DNA binding protein 43 (TDP-43) in Niemann-Pick disease type C. Acta Neuropathol Commun. 4 (1), 52.
DeJesus-Hernandez, M., Mackenzie, I.R., Boeve, B.F., Boxer, A.L., Baker, M., Rutherford, N.J., et al., 2011. Expanded GGGGCC hexanucleotide repeat in noncoding region of C9ORF72 causes chromosome 9p-linked FTD and ALS. Neuron. 72 (2), 245–256.
Demaegd, K., Schymkowitz, J., Rousseau, F., 2018. Transcellular spreading of tau in tauopathies. Chembiochem. 19 (23), 2424–2432.
Deshpande, A., Win, K.M., Busciglio, J., 2008. Tau isoform expression and regulation in human cortical neurons. FASEB J. 22 (7), 2357–2367.
Devlin, A.C., Burr, K., Borooah, S., Foster, J.D., Cleary, E.M., Geti, I., et al., 2015. Human iPSC-derived motoneurons harbouring TARDBP or C9ORF72 ALS mutations are dysfunctional despite maintaining viability. Nat. Commun. 6, 5999.
Dixit, R., Ross, J.L., Goldman, Y.E., Holzbaur, E.L.F., 2008. Differential regulation of dynein and kinesin motor proteins by tau. Science. 319 (5866), 1086.
Donnelly, C.J., Zhang, P.W., Pham, J.T., Haeusler, A.R., Mistry, N.A., Vidensky, S., et al., 2013. RNA toxicity from the ALS/FTD C9ORF72 expansion is mitigated by antisense intervention. Neuron. 80 (2), 415–428.
D'Souza, I., Poorkaj, P., Hong, M., Nochlin, D., Lee, V.M., Bird, T.D., et al., 1999. Missense and silent tau gene mutations cause frontotemporal dementia with parkinsonism-chromosome 17 type, by affecting multiple alternative RNA splicing regulatory elements. Proc. Natl. Acad. Sci. U. S. A. 96 (10), 5598–5603.
Egawa N, Kitaoka S, Tsukita K, Naitoh M, Takahashi K, Yamamoto T, et al. Drug screening for ALS using patient-specific induced pluripotent stem cells. Sci Transl Med. 2012;4(145):145ra04.
Ehrlich, M., Hallmann, A.L., Reinhardt, P., Arauzo-Bravo, M.J., Korr, S., Ropke, A., et al., 2015. Distinct neurodegenerative changes in an induced pluripotent stem cell model of frontotemporal dementia linked to mutant TAU protein. Stem Cell Reports. 5 (1), 83–96.
Elia, L.P., Mason, A.R., Alijagic, A., Finkbeiner, S., 2019. Genetic regulation of neuronal progranulin reveals a critical role for the autophagy-lysosome pathway. J. Neurosci. 39 (17), 3332–3344.
Esanov, R., Belle, K.C., van Blitterswijk, M., Belzil, V.V., Rademakers, R., Dickson, D.W., et al., 2016. C9orf72 promoter hypermethylation is reduced while hydroxymethylation is acquired during reprogramming of ALS patient cells. Exp. Neurol. 277, 171–177.
Espuny-Camacho, I., Arranz, A.M., Fiers, M., Snellinx, A., Ando, K., Munck, S., et al., 2017. Hallmarks of Alzheimer's disease in stem-cell-derived human neurons transplanted into mouse brain. Neuron. 93 (5), 1066–1081 (e8).
Esteras, N., Rohrer, J.D., Hardy, J., Wray, S., Abramov, A.Y., 2017. Mitochondrial hyperpolarization in iPSC-derived neurons from patients of FTDP-17 with 10+16 MAPT mutation leads to oxidative stress and neurodegeneration. Redox Biol. 12, 410–422.
Evans, L.D., Wassmer, T., Fraser, G., Smith, J., Perkinton, M., Billinton, A., et al., 2018. Extracellular monomeric and aggregated tau efficiently enter human neurons through overlapping but distinct pathways. Cell Rep. 22 (13), 3612–3624.
Evers, B.M., Rodriguez-Navas, C., Tesla, R.J., Prange-Kiel, J., Wasser, C.R., Yoo, K.S., et al., 2017. Lipidomic and transcriptomic basis of lysosomal dysfunction in progranulin deficiency. Cell Rep. 20 (11), 2565–2574.
Farg, M.A., Sundaramoorthy, V., Sultana, J.M., Yang, S., Atkinson, R.A., Levina, V., et al., 2014. C9ORF72, implicated in amytrophic lateral sclerosis and frontotemporal dementia, regulates endosomal trafficking. Hum. Mol. Genet. 23 (13), 3579–3595.
Ferraiuolo, L., Meyer, K., Sherwood, T.W., Vick, J., Likhite, S., Frakes, A., et al., 2016. Oligodendrocytes contribute to motor neuron death in ALS via SOD1-dependent mechanism. Proc. Natl. Acad. Sci. 113 (42), E6496–E6505.
Finch, N., Carrasquillo, M.M., Baker, M., Rutherford, N.J., Coppola, G., Dejesus-Hernandez, M., et al., 2011. TMEM106B regulates progranulin levels and the penetrance of FTLD in GRN mutation carriers. Neurology. 76 (5), 467–474.
Floris, G., Borghero, G., Cannas, A., Di Stefano, F., Murru, M.R., Corongiu, D., et al., 2015. Clinical phenotypes and radiological findings in frontotemporal dementia related to TARDBP mutations. J. Neurol. 262 (2), 375–384.
Fong, H., Wang, C., Knoferle, J., Walker, D., Balestra, M.E., Tong, L.M., et al., 2013. Genetic correction of tauopathy phenotypes in neurons derived from human induced pluripotent stem cells. Stem Cell Reports. 1 (3), 226–234.
Freibaum, B.D., Lu, Y., Lopez-Gonzalez, R., Kim, N.C., Almeida, S., Lee, K.H., et al., 2015. GGGGCC repeat expansion in C9orf72 compromises nucleocytoplasmic transport. Nature. 525 (7567), 129–133.
Gallagher, M.D., Suh, E., Grossman, M., Elman, L., McCluskey, L., Van Swieten, J.C., et al., 2014. TMEM106B is a genetic modifier of frontotemporal lobar degeneration with C9orf72 hexanucleotide repeat expansions. Acta Neuropathol. 127 (3), 407–418.
Gao, F.B., 2010. Context-dependent functions of specific microRNAs in neuronal development. Neural Dev. 5, 25.
Gao, X., Joselin, A.P., Wang, L., Kar, A., Ray, P., Bateman, A., et al., 2010. Progranulin promotes neurite outgrowth and neuronal differentiation by regulating GSK-3 beta.

Protein Cell. 1 (6), 552–562.
Garcia-Leon, J.A., Cabrera-Socorro, A., Eggermont, K., Swijsen, A., Terryn, J., Fazal, R., et al., 2018. Generation of a human induced pluripotent stem cell-based model for tauopathies combining three microtubule-associated protein TAU mutations which displays several phenotypes linked to neurodegeneration. Alzheimers Dement. 14 (10), 1261–1280.
Gascon, E., Lynch, K., Ruan, H., Almeida, S., Verheyden, J.M., Seeley, W.W., et al., 2014. Alterations in microRNA-124 and AMPA receptors contribute to social behavioral deficits in frontotemporal dementia. Nat. Med. 20 (12), 1444–1451.
Gass, J., Cannon, A., Mackenzie, I.R., Boeve, B., Baker, M., Adamson, J., et al., 2006. Mutations in progranulin are a major cause of ubiquitin-positive frontotemporal lobar degeneration. Hum. Mol. Genet. 15 (20), 2988–3001.
Gendron, T.F., Bieniek, K.F., Zhang, Y.J., Jansen-West, K., Ash, P.E., Caulfield, T., et al., 2013. Antisense transcripts of the expanded C9ORF72 hexanucleotide repeat form nuclear RNA foci and undergo repeat-associated non-ATG translation in c9FTD/ALS. Acta Neuropathol. 126 (6), 829–844.
Ghosh, S., Lippa, C.F., 2015. Clinical subtypes of frontotemporal dementia. Am. J. Alzheimers Dis. Other Dement. 30 (7), 653–661.
Gijselinck, I., Van Broeckhoven, C., Cruts, M., 2008. Granulin mutations associated with frontotemporal lobar degeneration and related disorders: an update. Hum. Mutat. 29 (12), 1373–1386.
Gijselinck, I., Van Langenhove, T., van der Zee, J., Sleegers, K., Philtjens, S., Kleinberger, G., et al., 2012. A C9orf72 promoter repeat expansion in a Flanders-Belgian cohort with disorders of the frontotemporal lobar degeneration-amyotrophic lateral sclerosis spectrum: a gene identification study. Lancet Neurol. 11 (1), 54–65.
Goedert, M., Jakes, R., 1990. Expression of separate isoforms of human tau protein: correlation with the tau pattern in brain and effects on tubulin polymerization. EMBO J. 9 (13), 4225–4230.
Goedert, M., Spillantini, M.G., Jakes, R., Rutherford, D., Crowther, R.A., 1989a. Multiple isoforms of human microtubule-associated protein tau: sequences and localization in neurofibrillary tangles of Alzheimer's disease. Neuron. 3 (4), 519–526.
Goedert, M., Spillantini, M.G., Potier, M.C., Ulrich, J., Crowther, R.A., 1989b. Cloning and sequencing of the cDNA encoding an isoform of microtubule-associated protein tau containing four tandem repeats: differential expression of tau protein mRNAs in human brain. EMBO J. 8 (2), 393–399.
Gotz, J., Chen, F., van Dorpe, J., Nitsch, R.M., 2001. Formation of neurofibrillary tangles in P301l tau transgenic mice induced by Abeta 42 fibrils. Science. 293 (5534), 1491–1495.
Gotz, J., Halliday, G., Nisbet, R.M., 2019. Molecular pathogenesis of the tauopathies. Annu. Rev. Pathol. 14, 239–261.
Gotzl, J.K., Mori, K., Damme, M., Fellerer, K., Tahirovic, S., Kleinberger, G., et al., 2014. Common pathobiochemical hallmarks of progranulin-associated frontotemporal lobar degeneration and neuronal ceroid lipofuscinosis. Acta Neuropathol. 127 (6), 845–860.
Gotzl JK, Brendel M, Werner G, Parhizkar S, Sebastian Monasor L, Kleinberger G, et al. Opposite microglial activation stages upon loss of PGRN or TREM2 result in reduced cerebral glucose metabolism. EMBO Mol Med. 2019;11(6).
Greaves, C.V., Rohrer, J.D., 2019. An update on genetic frontotemporal dementia. J. Neurol. 266 (8), 2075–2086.
Grenier, K., Kao, J., Diamandis, P., 2020. Three-dimensional modeling of human neurodegeneration: brain organoids coming of age. Mol. Psychiatry 25 (2), 254–274.
Grover, A., Houlden, H., Baker, M., Adamson, J., Lewis, J., Prihar, G., et al., 1999. 5′ splice site mutations in tau associated with the inherited dementia FTDP-17 affect a stem-loop structure that regulates alternative splicing of exon 10. J. Biol. Chem. 274 (21), 15134–15143.
Grover, A., DeTure, M., Yen, S.H., Hutton, M., 2002. Effects on splicing and protein function of three mutations in codon N296 of tau in vitro. Neurosci. Lett. 323 (1), 33–36.
Guillaumet-Adkins, A., Yanez, Y., Peris-Diaz, M.D., Calabria, I., Palanca-Ballester, C., Sandoval, J., 2017. Epigenetics and oxidative stress in aging. Oxidative Med. Cell. Longev. 2017, 9175806.
Guillozet, A.L., Weintraub, S., Mash, D.C., Mesulam, M.M., 2003. Neurofibrillary tangles, amyloid, and memory in aging and mild cognitive impairment. Arch. Neurol. 60 (5), 729–736.
Handel, A.E., Chintawar, S., Lalic, T., Whiteley, E., Vowles, J., Giustacchini, A., et al., 2016. Assessing similarity to primary tissue and cortical layer identity in induced pluripotent stem cell-derived cortical neurons through single-cell transcriptomics. Hum. Mol. Genet. 25 (5), 989–1000.
Hardy, J., 2017. The discovery of Alzheimer-causing mutations in the APP gene and the formulation of the "amyloid cascade hypothesis". FEBS J. 284 (7), 1040–1044.
Hartfield, E.M., Yamasaki-Mann, M., Ribeiro Fernandes, H.J., Vowles, J., James, W.S., Cowley, S.A., et al., 2014. Physiological characterisation of human iPS-derived dopaminergic neurons. PLoS One 9 (2), e87388.
Hasselmann, J., Blurton-Jones, M., 2020. Human iPSC-derived microglia: a growing toolset to study the brain's innate immune cells. Glia 68, 721–739.
Hefti, M.M., Kim, S., Bell, A.J., Betters, R.K., Fiock, K.L., Iida, M.A., et al., 2019. Tau phosphorylation and aggregation in the developing human brain. J. Neuropathol. Exp. Neurol. 78 (10), 930–938.
Ho, V.M., Dallalzadeh, L.O., Karathanasis, N., Keles, M.F., Vangala, S., Grogan, T., et al., 2014. GluA2 mRNA distribution and regulation by miR-124 in hippocampal neurons. Mol. Cell. Neurosci. 61, 1–12.
Holler, C.J., Taylor, G., McEachin, Z.T., Deng, Q., Watkins, W.J., Hudson, K., et al., 2016. Trehalose upregulates progranulin expression in human and mouse models of GRN haploinsufficiency: a novel therapeutic lead to treat frontotemporal dementia. Mol. Neurodegener. 11 (1), 46.
Holler CJ, Taylor G, Deng Q, Kukar T. Intracellular proteolysis of progranulin generates stable, lysosomal granulins that are haploinsufficient in patients with frontotemporal dementia caused by GRN mutations. eNeuro. 2017;4(4).
Hou, Q., Ruan, H., Gilbert, J., Wang, G., Ma, Q., Yao, W.D., et al., 2015. MicroRNA miR124 is required for the expression of homeostatic synaptic plasticity. Nat. Commun. 6, 10045.
Hu, F., Padukkavidana, T., Vaegter, C.B., Brady, O.A., Zheng, Y., Mackenzie, I.R., et al., 2010. Sortilin-mediated endocytosis determines levels of the frontotemporal dementia protein, progranulin. Neuron. 68 (4), 654–667.
Hutton, M., Lendon, C.L., Rizzu, P., Baker, M., Froelich, S., Houlden, H., et al., 1998. Association of missense and 5′-splice-site mutations in tau with the inherited dementia FTDP-17. Nature. 393 (6686), 702–705.
Imamura, K., Sahara, N., Kanaan, N.M., Tsukita, K., Kondo, T., Kutoku, Y., et al., 2016a. Calcium dysregulation contributes to neurodegeneration in FTLD patient iPSC-derived neurons. Sci. Rep. 6, 34904.
Imamura, K., Sahara, N., Kanaan, N.M., Tsukita, K., Kondo, T., Kutoku, Y., et al., 2016b. Calcium dysregulation contributes to neurodegeneration in FTLD patient iPSC-derived neurons. Sci. Rep. 6 (1), 34904.
Imamura K, Izumi Y, Watanabe A, Tsukita K, Woltjen K, Yamamoto T, et al. The Src/c-Abl pathway is a potential therapeutic target in amyotrophic lateral sclerosis. Sci Transl Med. 2017;9(391).
Iovino, M., Patani, R., Watts, C., Chandran, S., Spillantini, M.G., 2010. Human stem cell-derived neurons: a system to study human tau function and dysfunction. PLoS One 5 (11), e13947.
Iovino, M., Agathou, S., González-Rueda, A., Del Castillo, Velasco-Herrera M., Borroni, B., Alberici, A., et al., 2015. Early maturation and distinct tau pathology in induced pluripotent stem cell-derived neurons from patients with MAPT mutations. Brain. 138 (Pt 11), 3345–3359.
Iseki, E., Matsumura, T., Marui, W., Hino, H., Odawara, T., Sugiyama, N., et al., 2001. Familial frontotemporal dementia and parkinsonism with a novel N296H mutation in exon 10 of the tau gene and a widespread tau accumulation in the glial cells. Acta Neuropathol. 102 (3), 285–292.
Jayakumar, A.R., Tong, X.Y., Shamaladevi, N., Barcelona, S., Gaidosh, G., Agarwal, A., et al., 2017. Defective synthesis and release of astrocytic thrombospondin-1 mediates the neuronal TDP-43 proteinopathy, resulting in defects in neuronal integrity associated with chronic traumatic encephalopathy: in vitro studies. J. Neurochem. 140 (4), 645–661.
Jian, J., Tian, Q.Y., Hettinghouse, A., Zhao, S., Liu, H., Wei, J., et al., 2016. Progranulin recruits HSP70 to beta-glucocerebrosidase and is therapeutic against Gaucher disease. EBioMedicine. 13, 212–224.
Jiang, H., Mankodi, A., Swanson, M.S., Moxley, R.T., Thornton, C.A., 2004. Myotonic dystrophy type 1 is associated with nuclear foci of mutant RNA, sequestration of muscleblind proteins and deregulated alternative splicing in neurons. Hum. Mol. Genet. 13 (24), 3079–3088.
Jiang, S., Wen, N., Li, Z., Dube, U., Del Aguila, J., Budde, J., et al., 2018. Integrative system biology analyses of CRISPR-edited iPSC-derived neurons and human brains reveal deficiencies of presynaptic signaling in FTLD and PSP. Transl. Psychiatry 8 (1), 265.
Josephs, K.A., Hodges, J.R., Snowden, J.S., Mackenzie, I.R., Neumann, M., Mann, D.M., et al., 2011. Neuropathological background of phenotypical variability in frontotemporal dementia. Acta Neuropathol. 122 (2), 137–153.
Jovicic, A., Mertens, J., Boeynaems, S., Bogaert, E., Chai, N., Yamada, S.B., et al., 2015. Modifiers of C9orf72 dipeptide repeat toxicity connect nucleocytoplasmic transport defects to FTD/ALS. Nat. Neurosci. 18 (9), 1226–1229.
Kaplan, A., Spiller, K.J., Towne, C., Kanning, K.C., Choe, G.T., Geber, A., et al., 2014. Neuronal matrix metalloproteinase-9 is a determinant of selective neurodegeneration. Neuron. 81 (2), 333–348.
Kar, A., Kuo, D., He, R., Zhou, J., Wu, J.Y., 2005. Tau alternative splicing and frontotemporal dementia. Alzheimer Dis. Assoc. Disord. 19 (Suppl. 1), S29–S36.
Kara E, Ling H, Pittman AM, Shaw K, de Silva R, Simone R, et al. The MAPT p.A152T variant is a risk factor associated with tauopathies with atypical clinical and neuropathological features. Neurobiol Aging. 2012;33(9):2231 e7- e14.
Karch, C.M., Kao, A.W., Karydas, A., Onanuga, K., Martinez, R., Argouarch, A., et al., 2019. A comprehensive resource for induced pluripotent stem cells from patients with primary tauopathies. Stem Cell Reports. 13 (5), 939–955.
Ke, Y.D., Suchowerska, A.K., van der Hoven, J., De Silva, D.M., Wu, C.W., van Eersel, J., et al., 2012. Lessons from tau-deficient mice. Int. J. Alzheimers Dis. 2012, 873270.
Kessenbrock, K., Frohlich, L., Sixt, M., Lammermann, T., Pfister, H., Bateman, A., et al., 2008. Proteinase 3 and neutrophil elastase enhance inflammation in mice by inactivating antiinflammatory progranulin. J. Clin. Invest. 118 (7), 2438–2447.
Ketscher, A., Ketterer, S., Dollwet-Mack, S., Reif, U., Reinheckel, T., 2016. Neuroectoderm-specific deletion of cathepsin D in mice models human inherited neuronal ceroid lipofuscinosis type 10. Biochimie. 122, 219–226.
Ketterer, S., Gomez-Auli, A., Hillebrand, L.E., Petrera, A., Ketscher, A., Reinheckel, T., 2017. Inherited diseases caused by mutations in cathepsin protease genes. FEBS J. 284 (10), 1437–1454.
Kilpinen, H., Goncalves, A., Leha, A., Afzal, V., Alasoo, K., Ashford, S., et al., 2017. Common genetic variation drives molecular heterogeneity in human iPSCs. Nature. 546 (7658), 370–375.
Klein, Z.A., Takahashi, H., Ma, M., Stagi, M., Zhou, M., Lam, T.T., et al., 2017. Loss of TMEM106B ameliorates lysosomal and frontotemporal dementia-related phenotypes in progranulin-deficient mice. Neuron. 95 (2), 281–296 (e6).
Kosik, K.S., Orecchio, L.D., Bakalis, S., Neve, R.L., 1989. Developmentally regulated expression of specific tau sequences. Neuron. 2 (4), 1389–1397.
Kovacs, G.G., Murrell, J.R., Horvath, S., Haraszti, L., Majtenyi, K., Molnar, M.J., et al., 2009. TARDBP variation associated with frontotemporal dementia, supranuclear gaze palsy, and chorea. Mov. Disord. 24 (12), 1843–1847.

Krefft, O., Jabali, A., Iefremova, V., Koch, P., Ladewig, J., 2018. Generation of standardized and reproducible forebrain-type cerebral organoids from human induced pluripotent stem cells. J. Vis. Exp. 131.
Kreiter, N., Pal, A., Lojewski, X., Corcia, P., Naujock, M., Reinhardt, P., et al., 2018. Age-dependent neurodegeneration and organelle transport deficiencies in mutant TDP43 patient-derived neurons are independent of TDP43 aggregation. Neurobiol. Dis. 115, 167–181.
Lancaster, M.A., Knoblich, J.A., 2014. Generation of cerebral organoids from human pluripotent stem cells. Nat. Protoc. 9 (10), 2329–2340.
Lancaster, M.A., Renner, M., Martin, C.A., Wenzel, D., Bicknell, L.S., Hurles, M.E., et al., 2013. Cerebral organoids model human brain development and microcephaly. Nature. 501 (7467), 373–379.
Lashley, T., Rohrer, J.D., Mead, S., Revesz, T., 2015. Review: an update on clinical, genetic and pathological aspects of frontotemporal lobar degenerations. Neuropathol. Appl. Neurobiol. 41 (7), 858–881.
Le Ber, I., Camuzat, A., Guerreiro, R., Bouya-Ahmed, K., Bras, J., Nicolas, G., et al., 2013. SQSTM1 mutations in French patients with frontotemporal dementia or frontotemporal dementia with amyotrophic lateral sclerosis. JAMA neurology. 70 (11), 1403–1410.
Lee, Y.B., Chen, H.J., Peres, J.N., Gomez-Deza, J., Attig, J., Stalekar, M., et al., 2013. Hexanucleotide repeats in ALS/FTD form length-dependent RNA foci, sequester RNA binding proteins, and are neurotoxic. Cell Rep. 5 (5), 1178–1186.
Lee, W.C., Almeida, S., Prudencio, M., Caulfield, T.R., Zhang, Y.J., Tay, W.M., et al., 2014. Targeted manipulation of the sortilin-progranulin axis rescues progranulin haploinsufficiency. Hum. Mol. Genet. 23 (6), 1467–1478.
Lee, H.K., Velazquez Sanchez, C., Chen, M., Morin, P.J., Wells, J.M., Hanlon, E.B., et al., 2016. Three dimensional human neuro-spheroid model of Alzheimer's disease based on differentiated induced pluripotent stem cells. PLoS One 11 (9), e0163072.
Lee, C.W., Stankowski, J.N., Chew, J., Cook, C.N., Lam, Y.W., Almeida, S., et al., 2017. The lysosomal protein cathepsin L is a progranulin protease. Mol. Neurodegener. 12 (1), 55.
Levine, T.P., Daniels, R.D., Gatta, A.T., Wong, L.H., Hayes, M.J., 2013. The product of C9orf72, a gene strongly implicated in neurodegeneration, is structurally related to DENN Rab-GEFs. Bioinformatics. 29 (4), 499–503.
Lewis, J., Dickson, D.W., Lin, W.L., Chisholm, L., Corral, A., Jones, G., et al., 2001. Enhanced neurofibrillary degeneration in transgenic mice expressing mutant tau and APP. Science. 293 (5534), 1487–1491.
Lin, M.T., Beal, M.F., 2006. Mitochondrial dysfunction and oxidative stress in neurodegenerative diseases. Nature. 443 (7113), 787–795.
Liu, C., Gotz, J., 2013. Profiling murine tau with 0N, 1N and 2N isoform-specific antibodies in brain and peripheral organs reveals distinct subcellular localization, with the 1N isoform being enriched in the nucleus. PLoS One 8 (12), e84849.
Lopez-Gonzalez, R., Lu, Y., Gendron Tania, F., Karydas, A., Tran, H., Yang, D., et al., 2016. Poly(GR) in C9ORF72-related ALS/FTD compromises mitochondrial function and increases oxidative stress and DNA damage in iPSC-derived motor neurons. Neuron. 92 (2), 383–391.
Mackenzie, I.R., 2007. The neuropathology and clinical phenotype of FTD with progranulin mutations. Acta Neuropathol. 114 (1), 49–54.
Mackenzie, I.R., Neumann, M., 2016. Molecular neuropathology of frontotemporal dementia: insights into disease mechanisms from postmortem studies. J. Neurochem. 138 (Suppl. 1), 54–70.
Mackenzie, I.R., Munoz, D.G., Kusaka, H., Yokota, O., Ishihara, K., Roeber, S., et al., 2011. Distinct pathological subtypes of FTLD-FUS. Acta Neuropathol. 121 (2), 207–218.
Mackenzie, I.R., Frick, P., Neumann, M., 2014. The neuropathology associated with repeat expansions in the C9ORF72 gene. Acta Neuropathol. 127 (3), 347–357.
Madill, M., McDonagh, K., Ma, J., Vajda, A., McLoughlin, P., O'Brien, T., et al., 2017. Amyotrophic lateral sclerosis patient iPSC-derived astrocytes impair autophagy via non-cell autonomous mechanisms. Molecular Brain. 10 (1), 22.
Mandelkow, E.M., Stamer, K., Vogel, R., Thies, E., Mandelkow, E., 2003. Clogging of axons by tau, inhibition of axonal traffic and starvation of synapses. Neurobiol. Aging 24 (8), 1079–1085.
Marogianni C, Rikos D, Provatas A, Dadouli K, Ntellas P, Tsitsi P, et al. The role of C9orf72 in neurodegenerative disorders: a systematic review, an updated meta-analysis, and the creation of an online database. Neurobiol Aging. 2019;84:238.e25-.e34.
Marschallinger J, Iram T, Zardeneta M, Lee SE, Lehallier B, Haney MS, et al. Lipid-droplet-accumulating microglia represent a dysfunctional and proinflammatory state in the aging brain. Nat Neurosci. 2020.
Mason, A.R., Elia, L.P., Finkbeiner, S., 2017. The receptor-interacting serine/threonine protein kinase 1 (RIPK1) regulates progranulin levels. J. Biol. Chem. 292 (8), 3262–3272.
McAleese, K.E., Walker, L., Erskine, D., Thomas, A.J., McKeith, I.G., Attems, J., 2017. TDP-43 pathology in Alzheimer's disease, dementia with Lewy bodies and ageing. Brain Pathol. 27 (4), 472–479.
McCarthy, A., Lonergan, R., Olszewska, D.A., O'Dowd, S., Cummins, G., Magennis, B., et al., 2015. Closing the tau loop: the missing tau mutation. Brain. 138 (Pt 10), 3100–3109.
Mertens, J., Paquola, A.C.M., Ku, M., Hatch, E., Bohnke, L., Ladjevardi, S., et al., 2015. Directly reprogrammed human neurons retain aging-associated transcriptomic signatures and reveal age-related nucleocytoplasmic defects. Cell Stem Cell 17 (6), 705–718.
Meyer, K., Ferraiuolo, L., Miranda, C.J., Likhite, S., McElroy, S., Renusch, S., et al., 2014. Direct conversion of patient fibroblasts demonstrates non-cell autonomous toxicity of astrocytes to motor neurons in familial and sporadic ALS. Proc. Natl. Acad. Sci. U. S. A. 111 (2), 829–832.
Miguel, L., Rovelet-Lecrux, A., Feyeux, M., Frebourg, T., Nassoy, P., Campion, D., et al., 2019. Detection of all adult tau isoforms in a 3D culture model of iPSC-derived neurons. Stem Cell Res. 40, 101541.
Miller, J.D., Ganat, Y.M., Kishinevsky, S., Bowman, R.L., Liu, B., Tu, E.Y., et al., 2013. Human iPSC-based modeling of late-onset disease via progerin-induced aging. Cell Stem Cell 13 (6), 691–705.
Miyamoto, K., Kowalska, A., Hasegawa, M., Tabira, T., Takahashi, K., Araki, W., et al., 2001. Familial frontotemporal dementia and parkinsonism with a novel mutation at an intron 10+11-splice site in the tau gene. Ann. Neurol. 50 (1), 117–120.
Moore, S., Alsop, E., Lorenzini, I., Starr, A., Rabichow, B.E., Mendez, E., et al., 2019. ADAR2 mislocalization and widespread RNA editing aberrations in C9orf72-mediated ALS/FTD. Acta Neuropathol. 138 (1), 49–65.
Mori, K., Weng, S.M., Arzberger, T., May, S., Rentzsch, K., Kremmer, E., et al., 2013. The C9orf72 GGGGCC repeat is translated into aggregating dipeptide-repeat proteins in FTLD/ALS. Science. 339 (6125), 1335–1338.
Nagai, M., Re, D.B., Nagata, T., Chalazonitis, A., Jessell, T.M., Wichterle, H., et al., 2007. Astrocytes expressing ALS-linked mutated SOD1 release factors selectively toxic to motor neurons. Nat. Neurosci. 10 (5), 615–622.
Nakamura, M., Shiozawa, S., Tsuboi, D., Amano, M., Watanabe, H., Maeda, S., et al., 2019. Pathological progression induced by the frontotemporal dementia-associated R406W tau mutation in patient-derived iPSCs. Stem Cell Reports. 13 (4), 684–699.
Nelson, P.T., Alafuzoff, I., Bigio, E.H., Bouras, C., Braak, H., Cairns, N.J., et al., 2012. Correlation of Alzheimer disease neuropathologic changes with cognitive status: a review of the literature. J. Neuropathol. Exp. Neurol. 71 (5), 362–381.
Neumann, M., Sampathu, D.M., Kwong, L.K., Truax, A.C., Micsenyi, M.C., Chou, T.T., et al., 2006. Ubiquitinated TDP-43 in frontotemporal lobar degeneration and amyotrophic lateral sclerosis. Science. 314 (5796), 130–133.
Neumann, M., Mackenzie, I.R., Cairns, N.J., Boyer, P.J., Markesbery, W.R., Smith, C.D., et al., 2007. TDP-43 in the ubiquitin pathology of frontotemporal dementia with VCP gene mutations. J. Neuropathol. Exp. Neurol. 66 (2), 152–157.
Neumann, M., Kwong, L.K., Lee, E.B., Kremmer, E., Flatley, A., Xu, Y., et al., 2009. Phosphorylation of S409/410 of TDP-43 is a consistent feature in all sporadic and familial forms of TDP-43 proteinopathies. Acta Neuropathol. 117 (2), 137–149.
Nogales, E., 2000. Structural insights into microtubule function. Annu. Rev. Biochem. 69, 277–302.
Nonaka, T., Kametani, F., Arai, T., Akiyama, H., Hasegawa, M., 2009. Truncation and pathogenic mutations facilitate the formation of intracellular aggregates of TDP-43. Hum. Mol. Genet. 18 (18), 3353–3364.
Nordin, A., Akimoto, C., Wuolikainen, A., Alstermark, H., Jonsson, P., Birve, A., et al., 2015. Extensive size variability of the GGGGCC expansion in C9orf72 in both neuronal and non-neuronal tissues in 18 patients with ALS or FTD. Hum. Mol. Genet. 24 (11), 3133–3142.
O'Rourke, J.G., Bogdanik, L., Yanez, A., Lall, D., Wolf, A.J., Muhammad, A.K., et al., 2016. C9orf72 is required for proper macrophage and microglial function in mice. Science. 351 (6279), 1324–1329.
Paonessa, F., Evans, L.D., Solanki, R., Larrieu, D., Wray, S., Hardy, J., et al., 2019. Microtubules deform the nuclear membrane and disrupt nucleocytoplasmic transport in tau-mediated frontotemporal dementia. Cell Rep. 26 (3), 582–593 (e5).
Park, J., Wetzel, I., Marriott, I., Dreau, D., D'Avanzo, C., Kim, D.Y., et al., 2018. A 3D human triculture system modeling neurodegeneration and neuroinflammation in Alzheimer's disease. Nat. Neurosci. 21 (7), 941–951.
Pasca, A.M., Sloan, S.A., Clarke, L.E., Tian, Y., Makinson, C.D., Huber, N., et al., 2015. Functional cortical neurons and astrocytes from human pluripotent stem cells in 3D culture. Nat. Methods 12 (7), 671–678.
Patani, R., Lewis, P.A., Trabzuni, D., Puddifoot, C.A., Wyllie, D.J., Walker, R., et al., 2012. Investigating the utility of human embryonic stem cell-derived neurons to model ageing and neurodegenerative disease using whole-genome gene expression and splicing analysis. J. Neurochem. 122 (4), 738–751.
Pooler, A.M., Phillips, E.C., Lau, D.H., Noble, W., Hanger, D.P., 2013. Physiological release of endogenous tau is stimulated by neuronal activity. EMBO Rep. 14 (4), 389–394.
Poorkaj, P., Bird, T.D., Wijsman, E., Nemens, E., Garruto, R.M., Anderson, L., et al., 1998. Tau is a candidate gene for chromosome 17 frontotemporal dementia. Ann. Neurol. 43 (6), 815–825.
Porterfield, V., Khan, S.S., Foff, E.P., Koseoglu, M.M., Blanco, I.K., Jayaraman, S., et al., 2020. A three-dimensional dementia model reveals spontaneous cell cycle re-entry and a senescence-associated secretory phenotype. Neurobiol. Aging 90, 125–134.
Preza, E., Hardy, J., Warner, T., Wray, S., 2016. Review: induced pluripotent stem cell models of frontotemporal dementia. Neuropathol. Appl. Neurobiol. 42 (6), 497–520.
Rademakers, R., Cruts, M., van Broeckhoven, C., 2004. The role of tau (MAPT) in frontotemporal dementia and related tauopathies. Hum. Mutat. 24 (4), 277–295.
Rademakers, R., Baker, M., Gass, J., Adamson, J., Huey, E.D., Momeni, P., et al., 2007. Phenotypic variability associated with progranulin haploinsufficiency in patients with the common 1477C– > T (Arg493X) mutation: an international initiative. Lancet Neurol. 6 (10), 857–868.
Raitano, S., Ordovas, L., De Muynck, L., Guo, W., Espuny-Camacho, I., Geraerts, M., et al., 2015. Restoration of progranulin expression rescues cortical neuron generation in an induced pluripotent stem cell model of frontotemporal dementia. Stem Cell Reports. 4 (1), 16–24.
Raja, W.K., Mungenast, A.E., Lin, Y.T., Ko, T., Abdurrob, F., Seo, J., et al., 2016. Self-organizing 3D human neural tissue derived from induced pluripotent stem cells recapitulate Alzheimer's disease phenotypes. PLoS One 11 (9), e0161969.
Rapoport, M., Dawson, H.N., Binder, L.I., Vitek, M.P., Ferreira, A., 2002. Tau is essential to beta -amyloid-induced neurotoxicity. Proc. Natl. Acad. Sci. U. S. A. 99 (9), 6364–6369.
Ratti, A., Gumina, V., Lenzi, P., Bossolasco, P., Fulceri, F., Volpe, C., et al., 2020. Chronic stress induces formation of stress granules and pathological TDP-43 aggregates in

human ALS fibroblasts and iPSC-motoneurons. Neurobiol. Dis. 105051.
Renton, A.E., Majounie, E., Waite, A., Simon-Sanchez, J., Rollinson, S., Gibbs, J.R., et al., 2011. A hexanucleotide repeat expansion in C9ORF72 is the cause of chromosome 9p21-linked ALS-FTD. Neuron. 72 (2), 257–268.
Roberson, E.D., Scearce-Levie, K., Palop, J.J., Yan, F., Cheng, I.H., Wu, T., et al., 2007. Reducing endogenous tau ameliorates amyloid beta-induced deficits in an Alzheimer's disease mouse model. Science. 316 (5825), 750–754.
Rohrer, J.D., Guerreiro, R., Vandrovcova, J., Uphill, J., Reiman, D., Beck, J., et al., 2009. The heritability and genetics of frontotemporal lobar degeneration. Neurology. 73 (18), 1451–1456.
Rohrer, J.D., Lashley, T., Schott, J.M., Warren, J.E., Mead, S., Isaacs, A.M., et al., 2011. Clinical and neuroanatomical signatures of tissue pathology in frontotemporal lobar degeneration. Brain. 134 (Pt 9), 2565–2581.
Russ, J., Liu, E.Y., Wu, K., Neal, D., Suh, E., Irwin, D.J., et al., 2015. Hypermethylation of repeat expanded C9orf72 is a clinical and molecular disease modifier. Acta Neuropathol. 129 (1), 39–52.
Rutherford NJ, Heckman MG, Dejesus-Hernandez M, Baker MC, Soto-Ortolaza AI, Rayaprolu S, et al. Length of normal alleles of C9ORF72 GGGGCC repeat do not influence disease phenotype. Neurobiol Aging. 2012;33(12):2950 e5–7.
Sareen D, O'Rourke JG, Meera P, Muhammad AK, Grant S, Simpkinson M, et al. Targeting RNA foci in iPSC-derived motor neurons from ALS patients with a C9ORF72 repeat expansion. Sci Transl Med. 2013;5(208):208ra149.
Sato, C., Barthelemy, N.R., Mawuenyega, K.G., Patterson, B.W., Gordon, B.A., Jockel-Balsarotti, J., et al., 2018. Tau kinetics in neurons and the human central nervous system. Neuron. 97 (6), 1284–1298 (e7).
Schwarz TL. Mitochondrial trafficking in neurons. Cold Spring Harb Perspect Biol. 2013;5(6).
Sellier, C., Campanari, M.L., Julie Corbier, C., Gaucherot, A., Kolb-Cheynel, I., Oulad-Abdelghani, M., et al., 2016. Loss of C9ORF72 impairs autophagy and synergizes with polyQ Ataxin-2 to induce motor neuron dysfunction and cell death. EMBO J. 35 (12), 1276–1297.
Selvaraj, B.T., Livesey, M.R., Zhao, C., Gregory, J.M., James, O.T., Cleary, E.M., et al., 2018. C9ORF72 repeat expansion causes vulnerability of motor neurons to Ca(2+)-permeable AMPA receptor-mediated excitotoxicity. Nat. Commun. 9 (1), 347.
Serio, A., Bilican, B., Barmada, S.J., Ando, D.M., Zhao, C., Siller, R., et al., 2013. Astrocyte pathology and the absence of non-cell autonomy in an induced pluripotent stem cell model of TDP-43 proteinopathy. Proc. Natl. Acad. Sci. U. S. A. 110 (12), 4697–4702.
Shi, Y., Lin, S., Staats, K.A., Li, Y., Chang, W.H., Hung, S.T., et al., 2018. Haploinsufficiency leads to neurodegeneration in C9ORF72 ALS/FTD human induced motor neurons. Nat. Med. 24 (3), 313–325.
Shipton, O.A., Leitz, J.R., Dworzak, J., Acton, C.E., Tunbridge, E.M., Denk, F., et al., 2011. Tau protein is required for amyloid {beta}-induced impairment of hippocampal long-term potentiation. J. Neurosci. 31 (5), 1688–1692.
Sieben, A., Van Langenhove, T., Engelborghs, S., Martin, J.J., Boon, P., Cras, P., et al., 2012. The genetics and neuropathology of frontotemporal lobar degeneration. Acta Neuropathol. 124 (3), 353–372.
Silva, M.C., Cheng, C., Mair, W., Almeida, S., Fong, H., Biswas, M.H.U., et al., 2016. Human iPSC-derived neuronal model of tau-A152T frontotemporal dementia reveals tau-mediated mechanisms of neuronal vulnerability. Stem Cell Reports. 7 (3), 325–340.
Silva, M.C., Ferguson, F.M., Cai, Q., Donovan, K.A., Nandi, G., Patnaik, D., et al., 2019. Targeted degradation of aberrant tau in frontotemporal dementia patient-derived neuronal cell models. Elife. 8.
Simone, R., Balendra, R., Moens, T.G., Preza, E., Wilson, K.M., Heslegrave, A., et al., 2018. G-quadruplex-binding small molecules ameliorate C9orf72 FTD/ALS pathology in vitro and in vivo. EMBO molecular medicine. 10 (1), 22–31.
Sivadasan, R., Hornburg, D., Drepper, C., Frank, N., Jablonka, S., Hansel, A., et al., 2016. C9ORF72 interaction with cofilin modulates actin dynamics in motor neurons. Nat. Neurosci. 19 (12), 1610–1618.
Skibinski, G., Parkinson, N.J., Brown, J.M., Chakrabarti, L., Lloyd, S.L., Hummerich, H., et al., 2005. Mutations in the endosomal ESCRTIII-complex subunit CHMP2B in frontotemporal dementia. Nat. Genet. 37 (8), 806–808.
Smith, K.R., Damiano, J., Franceschetti, S., Carpenter, S., Canafoglia, L., Morbin, M., et al., 2012. Strikingly different clinicopathological phenotypes determined by progranulin-mutation dosage. Am. J. Hum. Genet. 90 (6), 1102–1107.
Spillantini, M.G., Murrell, J.R., Goedert, M., Farlow, M.R., Klug, A., Ghetti, B., 1998. Mutation in the tau gene in familial multiple system tauopathy with presenile dementia. Proc. Natl. Acad. Sci. U. S. A. 95 (13), 7737–7741.
Sposito, T., Preza, E., Mahoney, C.J., Seto-Salvia, N., Ryan, N.S., Morris, H.R., et al., 2015. Developmental regulation of tau splicing is disrupted in stem cell-derived neurons from frontotemporal dementia patients with the 10 + 16 splice-site mutation in MAPT. Hum. Mol. Genet. 24 (18), 5260–5269.
Sreedharan, J., Blair, I.P., Tripathi, V.B., Hu, X., Vance, C., Rogelj, B., et al., 2008. TDP-43 mutations in familial and sporadic amyotrophic lateral sclerosis. Science. 319 (5870), 1668–1672.
Suh, H.S., Choi, N., Tarassishin, L., Lee, S.C., 2012. Regulation of progranulin expression in human microglia and proteolysis of progranulin by matrix metalloproteinase-12 (MMP-12). PLoS One 7 (4), e35115.
Sullivan, P.M., Zhou, X., Robins, A.M., Paushter, D.H., Kim, D., Smolka, M.B., et al., 2016. The ALS/FTLD associated protein C9orf72 associates with SMCR8 and WDR41 to regulate the autophagy-lysosome pathway. Acta Neuropathol Commun. 4 (1), 51.
Takada, L.T., 2015. The genetics of monogenic frontotemporal dementia. Dement Neuropsychol. 9 (3), 219–229.
Takahashi, K., Yamanaka, S., 2006. Induction of pluripotent stem cells from mouse embryonic and adult fibroblast cultures by defined factors. Cell. 126 (4), 663–676.
Tanji, K., Zhang, H.X., Mori, F., Kakita, A., Takahashi, H., Wakabayashi, K., 2012. p62/sequestosome 1 binds to TDP-43 in brains with frontotemporal lobar degeneration with TDP-43 inclusions. J. Neurosci. Res. 90 (10), 2034–2042.
Tian, R., Gachechiladze, M.A., Ludwig, C.H., Laurie, M.T., Hong, J.Y., Nathaniel, D., et al., 2019. CRISPR interference-based platform for multimodal genetic screens in human iPSC-derived neurons. Neuron. 104 (2), 239–255 (e12).
Trabzuni, D., Wray, S., Vandrovcova, J., Ramasamy, A., Walker, R., Smith, C., et al., 2012. MAPT expression and splicing is differentially regulated by brain region: relation to genotype and implication for tauopathies. Hum. Mol. Genet. 21 (18), 4094–4103.
Uesaka, N., Abe, M., Konno, K., Yamazaki, M., Sakoori, K., Watanabe, T., et al., 2018. Retrograde signaling from progranulin to Sort1 counteracts synapse elimination in the developing cerebellum. Neuron. 97 (4), 796–805 (e5).
Ugolino, J., Ji, Y.J., Conchina, K., Chu, J., Nirujogi, R.S., Pandey, A., et al., 2016. Loss of C9orf72 enhances autophagic activity via deregulated mTOR and TFEB signaling. PLoS Genet. 12 (11), e1006443.
Valdez, C., Wong, Y.C., Schwake, M., Bu, G., Wszolek, Z.K., Krainc, D., 2017. Progranulin-mediated deficiency of cathepsin D results in FTD and NCL-like phenotypes in neurons derived from FTD patients. Hum. Mol. Genet. 26 (24), 4861–4872.
van Blitterswijk, M., Mullen, B., Nicholson, A.M., Bieniek, K.F., Heckman, M.G., Baker, M.C., et al., 2014. TMEM106B protects C9ORF72 expansion carriers against frontotemporal dementia. Acta Neuropathol. 127 (3), 397–406.
van Blitterswijk, M., Gendron, T.F., Baker, M.C., DeJesus-Hernandez, M., Finch, N.A., Brown, P.H., et al., 2015. Novel clinical associations with specific C9ORF72 transcripts in patients with repeat expansions in C9ORF72. Acta Neuropathol. 130 (6), 863–876.
van der Zee, J., Gijselinck, I., Dillen, L., Van Langenhove, T., Theuns, J., Engelborghs, S., et al., 2013. A pan-European study of the C9orf72 repeat associated with FTLD: geographic prevalence, genomic instability, and intermediate repeats. Hum. Mutat. 34 (2), 363–373.
Varcianna, A., Myszczynska, M.A., Castelli, L.M., O'Neill, B., Kim, Y., Talbot, J., et al., 2019. Micro-RNAs secreted through astrocyte-derived extracellular vesicles cause neuronal network degeneration in C9orf72 ALS. EBioMedicine. 40, 626–635.
Vera, E., Bosco, N., Studer, L., 2016. Generating late-onset human iPSC-based disease models by inducing neuronal age-related phenotypes through telomerase manipulation. Cell Rep. 17 (4), 1184–1192.
Verheyen, A., Diels, A., Reumers, J., Van Hoorde, K., Van den Wyngaert, I., van Outryve d'Ydewalle, C., et al., 2018. Genetically engineered iPSC-derived FTDP-17 MAPT neurons display mutation-specific neurodegenerative and neurodevelopmental phenotypes. Stem Cell Reports. 11 (2), 363–379.
Vierbuchen, T., Ostermeier, A., Pang, Z.P., Kokubu, Y., Sudhof, T.C., Wernig, M., 2010. Direct conversion of fibroblasts to functional neurons by defined factors. Nature. 463 (7284), 1035–1041.
Visvanathan, J., Lee, S., Lee, B., Lee, J.W., Lee, S.K., 2007. The microRNA miR-124 antagonizes the anti-neural REST/SCP1 pathway during embryonic CNS development. Genes Dev. 21 (7), 744–749.
Wainger, B.J., Kiskinis, E., Mellin, C., Wiskow, O., Han, S.S., Sandoe, J., et al., 2014. Intrinsic membrane hyperexcitability of amyotrophic lateral sclerosis patient-derived motor neurons. Cell Rep. 7 (1), 1–11.
Wang, J.Z., Xia, Y.Y., Grundke-Iqbal, I., Iqbal, K., 2013. Abnormal hyperphosphorylation of tau: sites, regulation, and molecular mechanism of neurofibrillary degeneration. J. Alzheimers Dis. 33 (Suppl. 1), S123–S139.
Ward ME, Chen R, Huang HY, Ludwig C, Telpoukhovskaia M, Taubes A, et al. Individuals with progranulin haploinsufficiency exhibit features of neuronal ceroid lipofuscinosis. Sci Transl Med. 2017;9(385).
Watts, G.D., Wymer, J., Kovach, M.J., Mehta, S.G., Mumm, S., Darvish, D., et al., 2004. Inclusion body myopathy associated with Paget disease of bone and frontotemporal dementia is caused by mutant valosin-containing protein. Nat. Genet. 36 (4), 377–381.
Watts, G.D., Thomasova, D., Ramdeen, S.K., Fulchiero, E.C., Mehta, S.G., Drachman, D.A., et al., 2007. Novel VCP mutations in inclusion body myopathy associated with Paget disease of bone and frontotemporal dementia. Clin. Genet. 72 (5), 420–426.
Webster, C.P., Smith, E.F., Bauer, C.S., Moller, A., Hautbergue, G.M., Ferraiuolo, L., et al., 2016. The C9orf72 protein interacts with Rab1a and the ULK1 complex to regulate initiation of autophagy. EMBO J. 35 (15), 1656–1676.
Westergard, T., Jensen, B.K., Wen, X., Cai, J., Kropf, E., Iacovitti, L., et al., 2016. Cell-to-cell transmission of dipeptide repeat proteins linked to C9orf72-ALS/FTD. Cell Rep. 17 (3), 645–652.
Williams, K.L., Fifita, J.A., Vucic, S., Durnall, J.C., Kiernan, M.C., Blair, I.P., et al., 2013. Pathophysiological insights into ALS with C9ORF72 expansions. J. Neurol. Neurosurg. Psychiatry 84 (8), 931–935.
Wils, H., Kleinberger, G., Pereson, S., Janssens, J., Capell, A., Van Dam, D., et al., 2012. Cellular ageing, increased mortality and FTLD-TDP-associated neuropathology in progranulin knockout mice. J. Pathol. 228 (1), 67–76.
Wren, M.C., Zhao, J., Liu, C.C., Murray, M.E., Atagi, Y., Davis, M.D., et al., 2015. Frontotemporal dementia-associated N279K tau mutant disrupts subcellular vesicle trafficking and induces cellular stress in iPSC-derived neural stem cells. Mol. Neurodegener. 10, 46.
Wright, D.K., Liu, S., van der Poel, C., McDonald, S.J., Brady, R.D., Taylor, L., et al., 2017. Traumatic brain injury results in cellular, structural and functional changes resembling motor neuron disease. Cereb. Cortex 27 (9), 4503–4515.
Wszolek, Z.K., Pfeiffer, R.F., Bhatt, M.H., Schelper, R.L., Cordes, M., Snow, B.J., et al., 1992. Rapidly progressive autosomal dominant parkinsonism and dementia with pallido-ponto-nigral degeneration. Ann. Neurol. 32 (3), 312–320.
Wu, J.W., Hussaini, S.A., Bastille, I.M., Rodriguez, G.A., Mrejeru, A., Rilett, K., et al., 2016. Neuronal activity enhances tau propagation and tau pathology in vivo. Nat. Neurosci. 19 (8), 1085–1092.
Xi, Z., Zinman, L., Moreno, D., Schymick, J., Liang, Y., Sato, C., et al., 2013.

Hypermethylation of the CpG island near the G4C2 repeat in ALS with a C9orf72 expansion. Am. J. Hum. Genet. 92 (6), 981–989.
Xi, Z., Rainero, I., Rubino, E., Pinessi, L., Bruni, A.C., Maletta, R.G., et al., 2014. Hypermethylation of the CpG-island near the C9orf72 G(4)C(2)-repeat expansion in FTLD patients. Hum. Mol. Genet. 23 (21), 5630–5637.
Xi, Z., Zhang, M., Bruni, A.C., Maletta, R.G., Colao, R., Fratta, P., et al., 2015. The C9orf72 repeat expansion itself is methylated in ALS and FTLD patients. Acta Neuropathol. 129 (5), 715–727.
Xiang, Y., Tanaka, Y., Patterson, B., Kang, Y.J., Govindaiah, G., Roselaar, N., et al., 2017. Fusion of regionally specified hPSC-derived organoids models human brain development and interneuron migration. Cell Stem Cell 21 (3), 383–398 (e7).
Yang, Y.M., Gupta, S.K., Kim, K.J., Powers, B.E., Cerqueira, A., Wainger, B.J., et al., 2013. A small molecule screen in stem-cell-derived motor neurons identifies a kinase inhibitor as a candidate therapeutic for ALS. Cell Stem Cell 12 (6), 713–726.
Yang, M., Liang, C., Swaminathan, K., Herrlinger, S., Lai, F., Shiekhattar, R., et al., 2016. A C9ORF72/SMCR8-containing complex regulates ULK1 and plays a dual role in autophagy. Sci. Adv. 2 (9), e1601167.
Yasuda, M., Takamatsu, J., D'Souza, I., Crowther, R.A., Kawamata, T., Hasegawa, M., et al., 2000. A novel mutation at position +12 in the intron following exon 10 of the tau gene in familial frontotemporal dementia (FTD-Kumamoto). Ann. Neurol. 47 (4), 422–429.
Yin, F., Banerjee, R., Thomas, B., Zhou, P., Qian, L., Jia, T., et al., 2010. Exaggerated inflammation, impaired host defense, and neuropathology in progranulin-deficient mice. J. Exp. Med. 207 (1), 117–128.
Yu, Y., Run, X., Liang, Z., Li, Y., Liu, F., Liu, Y., et al., 2009. Developmental regulation of tau phosphorylation, tau kinases, and tau phosphatases. J. Neurochem. 108 (6), 1480–1494.
Yu, C.E., Bird, T.D., Bekris, L.M., Montine, T.J., Leverenz, J.B., Steinbart, E., et al., 2010. The spectrum of mutations in progranulin: a collaborative study screening 545 cases of neurodegeneration. Arch. Neurol. 67 (2), 161–170.
Yuva-Aydemir, Y., Almeida, S., Krishnan, G., Gendron, T.F., Gao, F.-B., 2019. Transcription elongation factor AFF2/FMR2 regulates expression of expanded GGGGCC repeat-containing C9ORF72 allele in ALS/FTD. Nat. Commun. 10 (1), 5466.
Zhang, Y.J., Xu, Y.F., Dickey, C.A., Buratti, E., Baralle, F., Bailey, R., et al., 2007. Progranulin mediates caspase-dependent cleavage of TAR DNA binding protein-43. J. Neurosci. 27 (39), 10530–10534.
Zhang, Y.J., Gendron, T.F., Xu, Y.F., Ko, L.W., Yen, S.H., Petrucelli, L., 2010. Phosphorylation regulates proteasomal-mediated degradation and solubility of TAR DNA binding protein-43 C-terminal fragments. Mol. Neurodegener. 5, 33.
Zhang, Z., Almeida, S., Lu, Y., Nishimura, A.L., Peng, L., Sun, D., et al., 2013. Downregulation of microRNA-9 in iPSC-derived neurons of FTD/ALS patients with TDP-43 mutations. PLoS One 8 (10), e76055.
Zhang, K., Donnelly, C.J., Haeusler, A.R., Grima, J.C., Machamer, J.B., Steinwald, P., et al., 2015. The C9orf72 repeat expansion disrupts nucleocytoplasmic transport. Nature. 525 (7567), 56–61.
Zhao, C., Devlin, A.C., Chouhan, A.K., Selvaraj, B.T., Stavrou, M., Burr, K., et al., 2020. Mutant C9orf72 human iPSC-derived astrocytes cause non-cell autonomous motor neuron pathophysiology. Glia. 68 (5), 1046–1064.
Zhou, X., Paushter, D.H., Feng, T., Sun, L., Reinheckel, T., Hu, F., 2017. Lysosomal processing of progranulin. Mol. Neurodegener. 12 (1), 62.
Zhu, J., Nathan, C., Jin, W., Sim, D., Ashcroft, G.S., Wahl, S.M., et al., 2002. Conversion of proepithelin to epithelins: roles of SLPI and elastase in host defense and wound repair. Cell. 111 (6), 867–878.